

## **Supporting Information**

# **A General and Scalable DNA Nano-chip with Fully Localized Architecture Enables Biocomputing in Living cells and Precisely Induces Cell Apoptosis**

Jintao Yi, Tingting Chen\* and Jinghong Li\*

## Table of Contents

Experimental Procedures.....	S3
Figure S1. Agarose gel electrophoresis analysis of the comple ABC and its reaction with ssDNA.....	S7
Figure S2. Characterization of DNA origami.....	S8
Figure S3. Reaction performance of basic DNA units (the triple-stranded DNA complex ABC) on DNA origami.....	S9
Figure S4. Agarose gel electrophoresis analysis of the toehold mediated strand displacement reaction in AND logic design.....	S10
Figure S5. The optimizing the assembly distance between input and output DNA components on the AND logic nano-chip.....	S11
Figure S6. Time-dependent Cy5 fluorescence signals of the AND gate in nano-chip or discrete DNA circuit response to different inputs.....	S12
Figure S7. Agarose gel electrophoresis analysis of the toehold mediated strand displacement reaction in OR logic design.....	S13
Figure S8. The optimizing the assembly distance between input and output DNA components on the AND logic nano-chip.....	S14
Figure S9. Agarose gel electrophoresis analysis of the toehold mediated strand displacement reaction in AND-NOT logic design.....	S15
Figure S10. The optimizing the assembly distance between input and output DNA components on the AND-NOT logic nano-chip.....	S16
Figure S11. Design and performance of the general AND logic nano-chip using two microRNAs (-122a, -15a) as inputs.....	S17
Figure S12. Agarose gel electrophoresis analysis in general AND logic nano-chip using two microRNAs (-122a, -15a) as inputs.....	S18
Figure S13. Design and performance of the general OR logic nano-chip using two microRNAs (-122a, -15a) as inputs.....	S19
Figure S14. Agarose gel electrophoresis analysis in general OR logic nano-chip using two microRNAs (-122a, -15a) as inputs.....	S20
Figure S15. Design and performance of the general NOT-AND logic nano-chip using two microRNAs (-122a, -15a) as inputs.....	S21
Figure S16. Agarose gel electrophoresis analysis in general AND-NOT logic nano-chip using two microRNAs (-122a, -15a) as inputs.....	S22
Figure S17. Design and performance of the AND-OR logic nano-chip using three microRNAs (-122a, -15a and -17) as inputs.....	S23
Figure S18. Design and performance of the AND-NOT-AND logic nano-chip using three microRNAs (-122a, -15a and -30a) as inputs.....	S24
Figure S19. Design and performance of the OR-NOT-AND logic nano-chip using three microRNAs (-122a, -15a and -30a) as inputs.....	S25
Figure S20. Design and performance of the OR-OR-AND logic nano-chip using three microRNAs (-122a, -124a, -15a and -30a) as inputs.....	S26
Figure S21. Time-dependent Cy5 fluorescence signal of the S <sub>0</sub> circuit in nano-chip or discrete DNA circuit response to different inputs.....	S27
Figure S22. Time-dependent FAM fluorescence signal of the S <sub>1</sub> circuit in nano-chip or discrete DNA circuit response to different inputs.....	S28
Figure S23. The performance of different nano-chip in responding to inputs (miR-122a, miR-15, miR-17).....	S29
Figure S24. Design and performance of the scalable cross-selective nano-chip.....	S30
Figure S25. Agarose gel electrophoresis analysis in three-inputs AND nano-chip using two microRNAs (-21, -17 and -30a) as inputs.....	S31
Figure S26. Study on the stability of the nano-chip.....	S32
Figure S27. Cell viability of HEK293 cells after incubated with different concentrations of nano-chip.....	S33
Figure S28. Endo-lysosomal release of nano-chip in HeLa cells.....	S34
Figure S29. The relative expression levels of miRNAs in different cells.....	S35
Figure S30. The performance of nano-chip in HEK293 cell.....	S36
Figure S31. CLSM images of HEK293 cells after pre-treated with different miRNA mimics.....	S37
Figure S32. The relative expression levels of miRNAs in HeLa cells after treated with different miRNA inhibitors.....	S38
Figure S33. The performance of nano-chip in Hela cells.....	S39
Figure S34. CLSM images of Hela cells after treatment with nano-chip or discrete DNA logic components.....	S40
Figure S35. The expression levels of Bcl-2 in HEK293 cells after different treatment.....	S41
Figure S36. Analyzing apoptosis of Hela cells after different treatments.....	S42
Figure S37. CLSM images of apoptosis in HEK293 cells after different treatments.....	S43
Figure S38. The wiring instructions of the AND logic gate with different assembly distance.....	S44
Figure S39. The wiring instructions of the OR logic gate with different assembly distance.....	S45
Figure S40. The wiring instructions of the AND-NOT logic gate with different assembly distance.....	S46
Figure S41. The wiring instructions of three basic logic gates on DNA origami.....	S47
Figure S42. The wiring instructions of complex DNA cascade circuits on the basis of the basic AND nano-chip.....	S48
Figure S43. The wiring instructions of complex DNA cascade circuits on the basis of the basic OR nano-chip.....	S49
Figure S44. The wiring instructions of the scalable nano-chip for multi-levels logic cascading and parallel biocomputing.....	S50
Figure S45. The wiring instructions of the three layers of cascade logic units on the nano-chip for intracellular molecular biocomputing.....	S51
Table S1. Sequence of oligonucleotides used in modular logic units.....	S52
Table S2. Sequence of oligonucleotides used to synthesize DNA origami.....	S53

## Experimental Procedures

### Materials and Reagents

Acetic acid, Magnesium acetate, EDTA and Tris base were purchased from Sigma-Aldrich (St. Louis, MO, USA). RIPA Lysis buffer, PMSF and BCA protein assay kit were obtained from Beyotime Biotechnology (Shanghai, China). Cell Counting Kit 8 was provided by Dojindo Laboratories (Kumamoto, Japan). Anti-bcl2 antibody, anti- $\beta$ -actin antibody, Alexa Fluor 488 annexin V, PI dead cell apoptosis kit, LysoTracker Red DND-99, bisbenzimidazole H 33342 trihydrochloride (Hoechst 33342), RPMI 1640 medium, fetal bovine serum, Dulbecco's modified Eagle's medium (DMEM), streptomycin and penicillin were obtained from Thermo Fisher Scientific Inc. (MA, USA). HeLa cells and HEK293 cells were provided by the cell bank of Central Laboratory at Xiangya Hospital (Changsha, China). microOFFTMhsa-miR-30a-5p inhibitors, microOFF hsa-miR-21-5p inhibitor and microOFF rno-miR-17-5p inhibitor were purchased from RiboBio Company (Guangzhou, China). M13mp18 was purchased from New England Biolabs (NEB, Ipswich, MA, USA). All other chemicals were of analytical grade and purchased from Sinopharm Chemical Reagent Co. Ltd. (Shanghai, China). All solutions were prepared by using ultrapure water, which was obtained through a Millipore Milli-Q water purification system (Billerica, MA, USA), with an electric resistance of  $>18.2$  M $\Omega$ . All DNA oligonucleotides (listed in Table S1 and Table S2) were synthesized and purified by HPLC by Sangon Biological Engineering Technology (Shanghai, China).

### Apparatus.

The fluorescence spectra were recorded using Fluorescence Spectrometer FS5 (Edinburgh Instruments, UK). With a 900 V PMT voltage, the excitation and emission slit were set at 5.0 nm. The gel image was obtained via a Tanon 4200SF gel imaging system (Tanon Science & Technology Co., Ltd., China). Atomic force microscopy (AFM) images of samples were measured on a Multimode 8 (Bruker, USA). The flow cytometric analysis was carried on the CytoFLEX flow cytometry system (Beckman, USA). The cell viability was evaluated by a microplate reader (ELx800, BioTek, USA). The fluorescence kinetics experiments were carried out on BIO-RAD PCR instruments (USA). All fluorescence imaging was measured on a confocal laser scanning fluorescence microscope (Nikon, Japan).

### Agarose Gel Electrophoresis.

All samples were prepared in advance. The triple-stranded DNA complex (named ABC) and all the duplex DNA complex (such as AR, BR, and DR etc.) were respectively prepared at 10  $\mu$ M through mixing each DNA strands with an equal concentration and annealing from 90°C to room temperature in 1 $\times$ TAE buffer (40 mM Tris base, 20 mM Acetic acid, 2 mM EDTA and 12.5 mM Magnesium acetate, pH 8.0). In the gel electrophoresis assay of the DNA strand displacement reactions, 10  $\mu$ L mixture solution containing 1  $\mu$ L of 10  $\mu$ M ABC, 1  $\mu$ L of 10  $\mu$ M A<sub>in-1</sub>, 1  $\mu$ L of 10  $\mu$ M B<sub>in-1</sub> or other given DNA strands was incubated in 1 $\times$ TAE buffer at 37°C for 2 h, then the obtained samples were mixed with 2  $\mu$ L of 6 $\times$ loading buffer and performed on 4% (w/v) agarose gel.

To assess the stability of DNA origami logic chip in complex conditions, 50 nM DNA origami logic chip was dispersed in 10  $\mu$ L of RPMI-1640 (Gibco) medium including fetal bovine serum (10% (v/v), FBS) or 10  $\mu$ L of cell lysates (0.5 mL, 1 $\times$ 10<sup>6</sup> cells mL<sup>-1</sup>) at 37°C for different times (0, 6, 12, 18, 24, 30, 36, 42, 48, 54, 60 and 72 h). Each sample was mixed with 2  $\mu$ L of 6 $\times$ loading buffer and carried out on 1% (w/v) agarose gel.

All the gel electrophoresis assays were performed in 1 $\times$ Tris-borate-EDTA (TBE) buffer (90 mM Tris-HCl, 2 mM EDTA, 90 mM boric acid and pH 8.0) at 110 V for 2 h at room temperature.

### Synthesis of DNA Origami and Preparation of the DNA Origami Logic Chip

DNA origami was synthesized according to the previous reported literature. The mixture solution containing 20  $\mu\text{L}$  of 100 nM M13mp18 scaffold and 80  $\mu\text{L}$  of 1  $\mu\text{M}$  helper strands (including staple strands and capture strands for triple-stranded or duplex DNA complex loading) was annealed in 200  $\mu\text{L}$  of 1 $\times$ TAE buffer by slowly cooling from 95°C to 25°C through PCR instrument more than 12 h. After that, the resulting solution was centrifuged at 7000g by using 100 kDa MWCO centrifuge filters for three times to remove the additional helper strands. The obtained solution was re-suspended with 1 $\times$ TAE buffer to stock concentrations of 20 nM and stored at 4°C for future using.

The DNA origami logic chip was prepared by incubating 100  $\mu\text{L}$  of 20 nM DNA origami with 20  $\mu\text{L}$  of 1  $\mu\text{M}$  each DNA logic components (including the triple-stranded DNA complex and the other duplex DNA complex) in 200  $\mu\text{L}$  of 1 $\times$ TAE buffer at 37°C for 2 h. After that, the additional DNA strands were removed by 100 kDa MWCO centrifuge filters for three times. The obtained solution was re-suspended with 1 $\times$ TAE buffer to stock concentrations of 20 nM and stored at 4°C for future using.

### **In Vitro Biocomputing of the DNA Origami Logic Chip**

In a typical fluorescence response assay of the DNA origami logic chip, 50  $\mu\text{L}$  reaction mixture containing 40 nM DNA origami logic chip and 200 nM of different input targets was incubated at 37°C for 330min and monitored its fluorescence signal on the real-time fluorescence quantitative PCR instrument.

To compare the kinetic profiles of different samples, the fluorescence intensity at each time point was normalized to the maximum fluorescence intensity observed within that sample during the assay period (expressed as a percentage of the maximum).

### **Cell Culture and Fluorescence Imaging**

HeLa cells and HEK293 cells were cultured in RPMI-1640 (Gibco) medium supplemented with 10% fetal bovine serum, streptomycin (100  $\mu\text{g mL}^{-1}$ ) and penicillin (100 units  $\text{mL}^{-1}$ ). All the cells were cultured in a humidified atmosphere (95 % air and 5 %  $\text{CO}_2$ ) at the temperature of 37°C. Before incubated with cell, the DNA origami logic chip should be concentrated to be 100 nM in cold PBS by using 100 kDa MWCO centrifuge filters.

For the biocomputing in the living cells, HEK293 cells (0.5 mL,  $1 \times 10^6$  cells  $\text{mL}^{-1}$ ) was seeded in a 35-mm confocal dish with 10 mm well and cultured in 2 mL RPMI-1640 medium for 24 h at 37°C. Then, cells were incubated with 250  $\mu\text{L}$  of culture medium containing 300 nM of different input targets and 3  $\mu\text{L}$  Lipo3000 at 37°C for 2 h, followed by incubating with 50 nM DNA origami logic chip and 3  $\mu\text{L}$  Lipo3000 in culture medium at 37°C for another 4 h. Subsequently, the cells were washed three times with cold phosphate buffer saline (PBS) and stained with Hoechst 33342 (10  $\mu\text{g/mL}$ ) for 10 min at 37°C before imaging.

For the cell identification, HeLa cells or HEK293 cells (0.5 mL,  $1 \times 10^6$  cells  $\text{mL}^{-1}$ ) was seeded in a 35-mm confocal dish with 10 mm well and cultured in 2 mL RPMI-1640 medium for 24 h at 37°C. Then, cells were incubated with 250  $\mu\text{L}$  of culture medium containing 50 nM DNA origami logic chip and 3  $\mu\text{L}$  Lipo3000 at 37°C for 4 h. Subsequently, the cells were washed and stained with Hoechst 33342 before imaging.

For the fluorescence imaging of miRNAs inhibition, HeLa cells were pretreat with 250  $\mu\text{M}$  miRNA inhibitors (including MicrOFFTMhsa-miR-30a-5p inhibitor, micrOFF hsa-miR-21-5p inhibitor and micrOFF rno-miR-17-5p inhibitor, respectively) and 6  $\mu\text{L}$  Lipo3000 in 1 mL culture medium at 37°C for 24 h. Then, the cells were incubated with DNA origami logic chip, washed three times with cold PBS and stained with Hoechst 33342 before imaging.

For the fluorescence imaging of bcl-2 silencing, the cells were treated with the given reagents at 37°C for 4 h, and kept culturing in RPMI-1640 medium for another 24 h. After that, the cells were fixed in 4% paraformaldehyde for 20 min, treated 0.2% Triton X-100 for permeabilization, and added 5% BSA for another 30 min at room temperature. Subsequently, the cells were successively incubated with 2  $\mu\text{g mL}^{-1}$  anti-bcl-2 antibodies and 4  $\mu\text{g mL}^{-1}$  the secondary antibodies of m-IgGk BP-CFL 488 in 1×PBS (6.7 mM, pH 7.4) at room temperature for 1 h, followed by washing with 1×PBS before imaging.

All fluorescence images were acquired by using an oil dipping objective (60×) on a Nikon confocal laser scanning fluorescence microscope at a sampling speed of 6.2 pixel/dwell and a size of 1024.

### **Determination of Cell Viability**

HeLa cells or HEK293 cells ( $5 \times 10^3$  cells) were seed on 96-well plates in the RPMI 1640 medium for 24 h under 5 wt %/vol CO<sub>2</sub> atmosphere. Subsequently, the cells were treated with different concentrations of DNA origami logic chip (0, 40, 80, 100, 150, 200 nM) for 24 h. Subsequently, the cells were washed twice with cold PBS and incubated with 100  $\mu\text{L}$  culture medium containing 10  $\mu\text{L}$  of CCK-8 stored solution at 37°C for another 2 h. Finally, the absorbance at 450 nm was measured on a microplate reader to calculate the cell viability.

### **Western Blot Analysis**

HeLa cells or HEK293 cells (0.5 mL,  $1 \times 10^6$  cells mL<sup>-1</sup>) were incubated with the given DNA origami logic chip at 37°C for 4 h, and kept culturing in RPMI-1640 medium for another 24 h. Subsequently, the cells were collected and lysed in 75  $\mu\text{L}$  of lysis buffer (50 mM Tris, 150 mM NaCl, 1% Triton X-100, 1% sodium deoxycholate, 5 mM EDTA, 1 mM PMSF, 0.1% SDS, 2  $\mu\text{g mL}^{-1}$  each of sodium orthovanadate, sodium fluoride, leupeptin and pH 7.4) at 4 °C for 30min. Then the lysate was centrifuged at 13000 g for 15 min to collected the supernatant. The concentration of total cellular proteins in the supernatant was determined by using BCA protein assay kit. Next, the total cellular proteins were separated and transferred to PVDF membranes. After incubated with anti-bcl-2 antibodies and secondary antibodies, the membranes were sent to detection on Gel Imaging System (Bio-RAD).

### **Flow Cytometry Experiments**

HeLa cells (0.5 mL,  $1 \times 10^6$  cells mL<sup>-1</sup>) were seeded in a 35-mm dish and cultured in RPMI-1640 medium at 37°C for 24 h. Subsequently, the cells were incubated with the given reagents, then treated with 0.25% trypsin for 2 min and centrifuged at 1000 g for 5 min followed by washing with PBS twice. Finally, the cells were re-dispersed in 500  $\mu\text{L}$  of cold PBS for flow cytometric analysis on a Cytotflex flow cytometry system.

For apoptosis analysis, the cells (0.5 mL,  $1 \times 10^6$  cells mL<sup>-1</sup>) were incubated with the given reagents for 4 h at 37°C. Then the cells were washed twice with cold PBS and continue cultured in RPMI-1640 medium for 24 h. After that, the cells were treated with 2  $\mu\text{g mL}^{-1}$  Alexa Fluor 488 annexin V and 10  $\mu\text{g mL}^{-1}$  PI dye in 1 mL cold PBS at room temperature for 15 min. Then cells were re-suspended in 1 mL cold PBS followed by flow cytometry assay with FITC and PI channel.

### **Real-Time Reverse Transcriptase-PCR Analysis**

HeLa cells or HEK293 cells (0.5 mL,  $1 \times 10^6$  cells mL<sup>-1</sup>) were seeded in a 35-mm dish, cultured in 3 mL RPMI-1640 medium for 24 h at 37°C, and incubated with the given reagents for 4 h at 37°C. Then the cells were washed twice with cold PBS and continue cultured in RPMI-1640 medium for 24 h. After that, the cells were treated with the given reagents. After 24 h cultivation, the total cellular RNAs were extracted from HeLa cells by using Uniq-10 column Trizol total RNA extraction kit (Sangon) according to the manufacturer's instructions. The cDNA samples were prepared with Revert Aid Premium Reverse Transcriptase (Thermo Fisher Scientific)

according to the indicated protocol. The analysis of cDNA was performed with SybrGreen PCR Master Mix (ABI, USA) on an ABI StepOnePlus qPCR instrument. The 20  $\mu$ L reaction solution contained 2  $\mu$ L cDNA sample, 10  $\mu$ L of SG Fast qPCR Master Mix (High Rox, 2 $\times$ ), 0.4  $\mu$ L of primer forward (10  $\mu$ M), 0.4  $\mu$ L of primer reverse (10  $\mu$ M) and 7.2  $\mu$ L of the nuclease-free water. The PCR conditions were as follows: an initial 95°C for 3 min followed by 40 cycles for 15 s at 95°C, for 20 s at 57°C and for 30 s at 72°C. The endogenous beta-actin mRNA was used as control for quantifying the relative level of bcl-2 mRNA. The target miRNAs were absolutely quantified by using fluorescent quantitative PCR method. The primers for bcl-2 used as follow: bcl-2 forward primer, 5'-gctggattataactcctctctttc-3'; bcl-2 reverse primer, 5'-ctctgcgacagcttataatggat-3'. The primers for miRNA-21 used as follow: miRNA-21 forward primer, 5'-acactccagctgggtagcttatcagact-3'; miRNA-21 reverse primer, 5'-ctcaactggtgctggtgagtcggcaattcagttgagctcaacatc-3'. The primers for miRNA17 used as follow: miRNA-17 forward primer, 5'-acactccagctgggcaaagtgcttacagtg-3'; miRNA-17 reverse primer, 5'-ctcaactggtgctggtgagtcggcaattcagttgagctacctg-3'. The primers for miRNA-30a used as follow: miRNA-30a forward primer, 5'-acactccagctgggtgtaaacaatcctcg-3'; miRNA-30a reverse primer, 5'-ctcaactggtgctggtgagtcggcaattcagttgagcttccagt-3'.



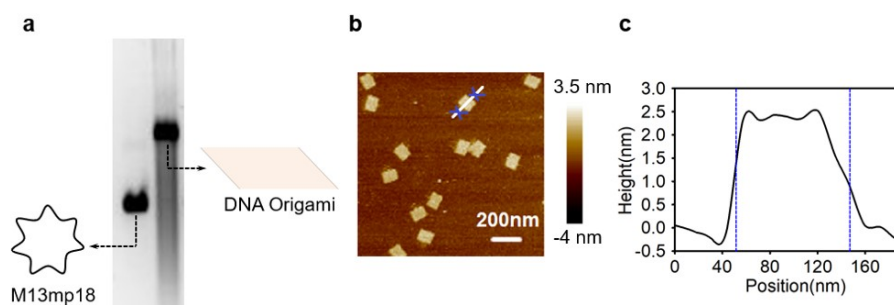


**Figure S2.** (a) Agarose gel electrophoresis analysis of the DNA origami. (b) Atomic force microscopy (AFM) image of the DNA origami. (c) Height profile of a cross-section of origami. The height of DNA origami is 2 nm.

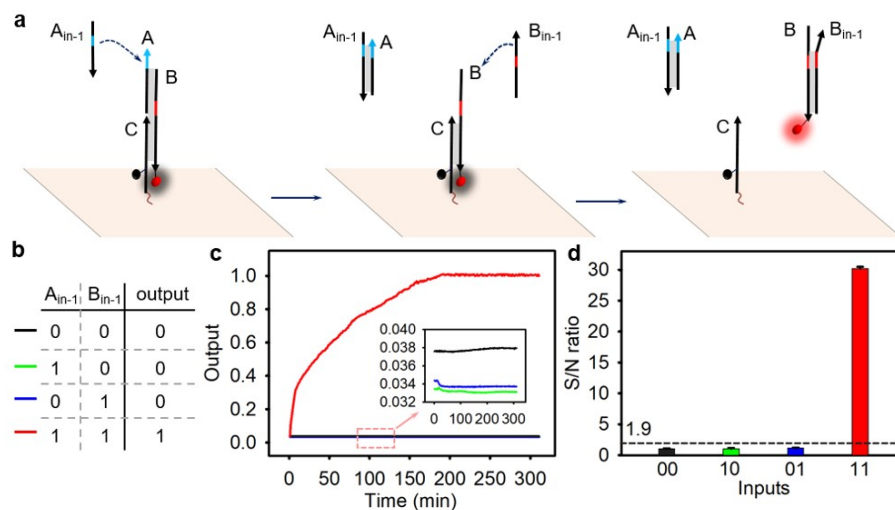


**Figure S3.** Reaction performance of basic DNA units (the triple-stranded DNA complex ABC) on DNA origami. (a) Schematic illustration of the triple-stranded DNA complex reacted with ssDNA  $A_{in-1}$  and  $B_{in-1}$ . (b) The truth value table of the logic reactions. (c) Time-dependent Cy5 fluorescence signals (output) of the triple-stranded DNA complex ABC response to different inputs. (d) Fluorescence intensity of the triple-stranded DNA complex ABC response to different inputs after 200 min of reaction. The true/false threshold (1/0) was calculated to be 1.9, which was the mean maximum value of false outputs plus 10 times of its standard deviation. The error bars indicate mean  $\pm$  standard deviation (SD,  $n = 5$ ).

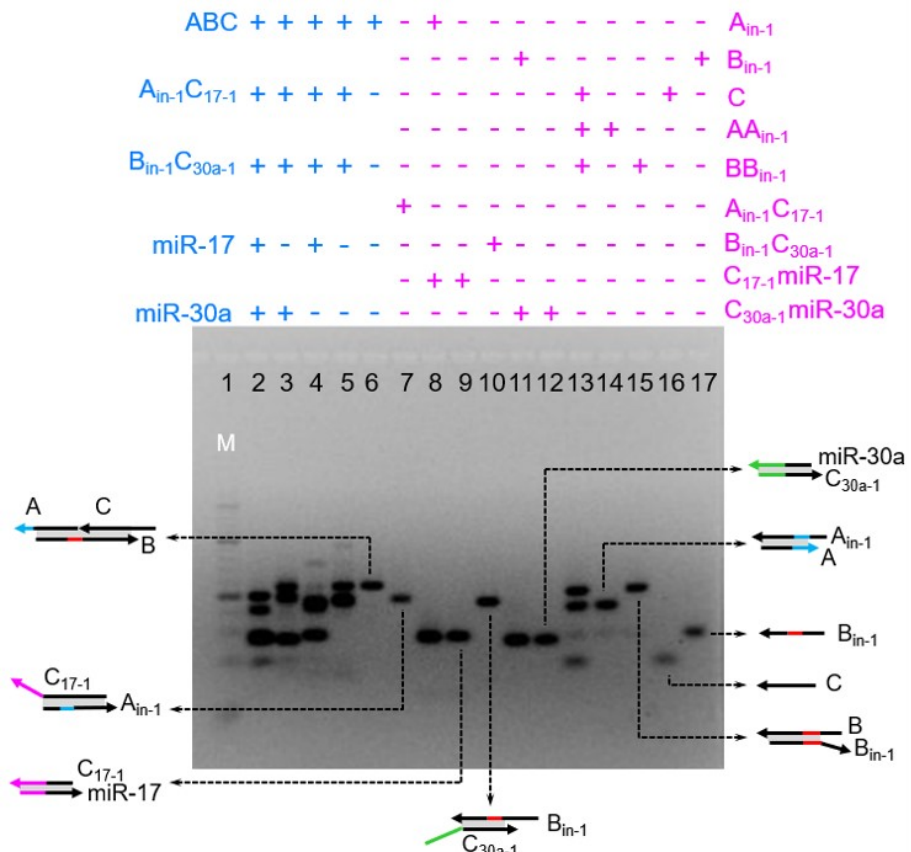


**Figure S4.** Agarose gel electrophoresis analysis of the toehold mediated strand displacement reaction between inputs (miRNA-17 and miRNA-30a) and the functional DNA units, including two DNA duplex  $A_{in-1}C_{17-1}$ ,  $B_{in-1}C_{30a-1}$  and the triple-stranded complex ABC. Lane 2-6 showed the products of the reactions between inputs and the functional DNA units marked in blue words. Lane 7-17 exhibited the products of the corresponding ssDNA and DNA duplexes marked in purple-red words.

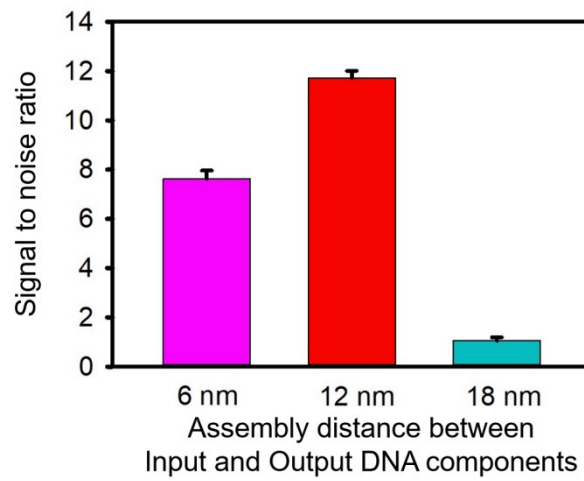


**Figure S5.** The optimizing the assembly distance between input and output DNA components on the AND logic nano-chip. The error bars indicate mean  $\pm$  standard deviation (SD, n = 5). The more detailed descriptions about wiring instructions were given in Figure S43.

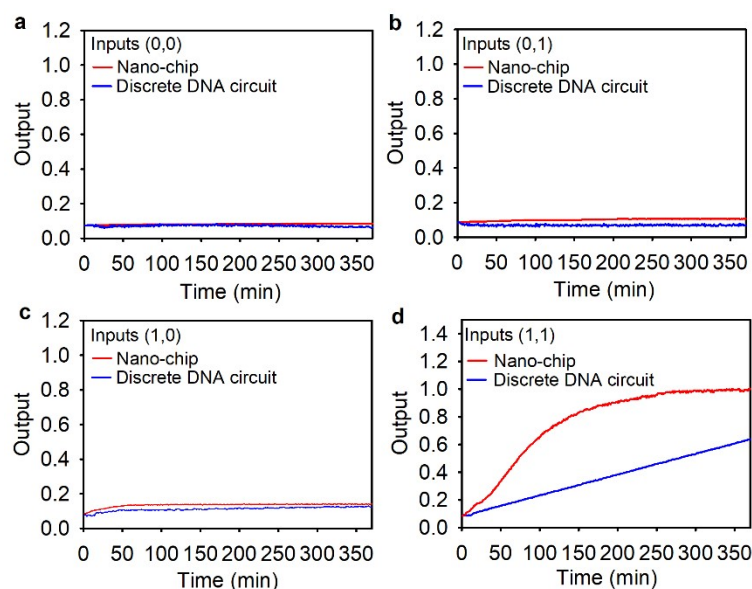


**Figure S6.** Time-dependent Cy5 fluorescence signals (output) of the AND gate in nano-chip or discrete DNA circuit response to different inputs (miRNA-17 and miRNA 30a). (a) The basic fluorescence signals of AND gate in nano-chip or discrete DNA circuit without incubation of miRNAs [Inputs(0,0)]; (b) the fluorescence signals of AND gate in nano-chip or discrete DNA circuit incubated only miRNA-30a [Inputs(0,1)]; (c) the fluorescence signals of AND gate in nano-chip or discrete DNA circuit incubated with only miRNA-17 [Inputs(1,0)]; (d) the fluorescence signals of AND gate in nano-chip or discrete DNA circuit incubated with both two miRNAs [Inputs(1,1)]. Red lines represented the fluorescence signals of AND gate in nano-chip responded to inputs, blue lines represented the fluorescence signals of AND gate in discrete DNA circuit responded to inputs. The data were further fitted to a first-order kinetic model, and the kinetic rate constant was  $0.0013 \text{ min}^{-1}$  and  $0.0303 \text{ min}^{-1}$  for the diffusible system and nano-chip, respectively.

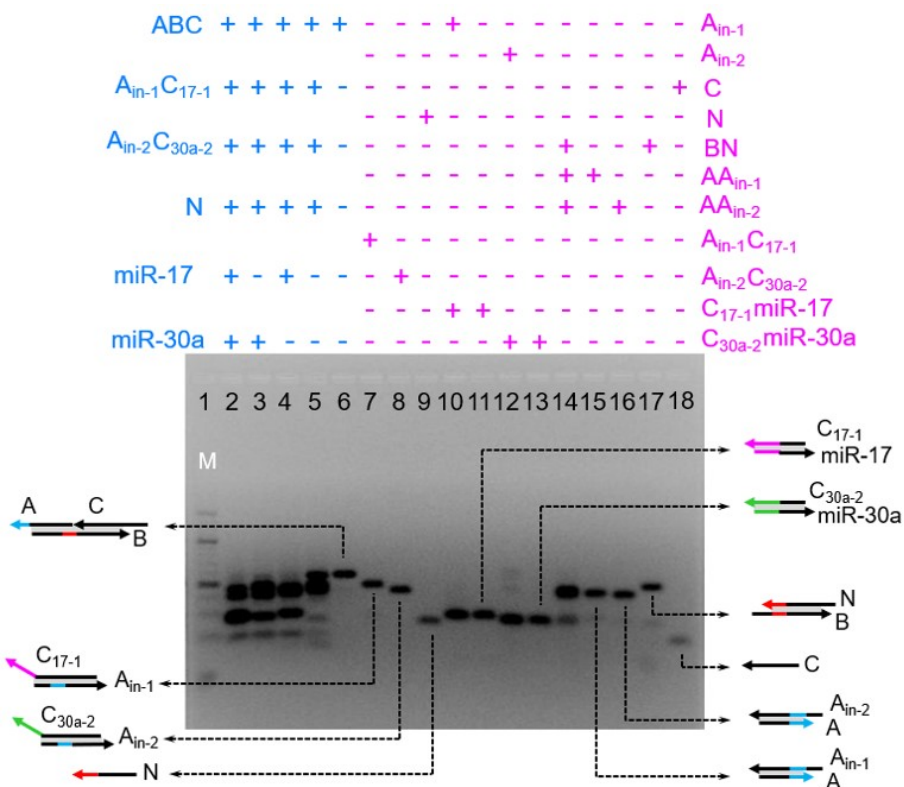


**Figure S7.** Agarose gel electrophoresis analysis of the toehold mediated strand displacement reaction between inputs (miRNA-17 and miRNA-30a) and the functional DNA units, including ssDNA N, two DNA duplex  $A_{in-1}C_{17-1}$ ,  $A_{in-2}C_{30a-2}$  and the triple-stranded complex ABC. Lane 2-6 showed the products of the reactions between inputs and the functional DNA units marked in blue words. Lane 7-18 exhibited the products of the corresponding ssDNA and DNA duplexes marked in purple-red words.

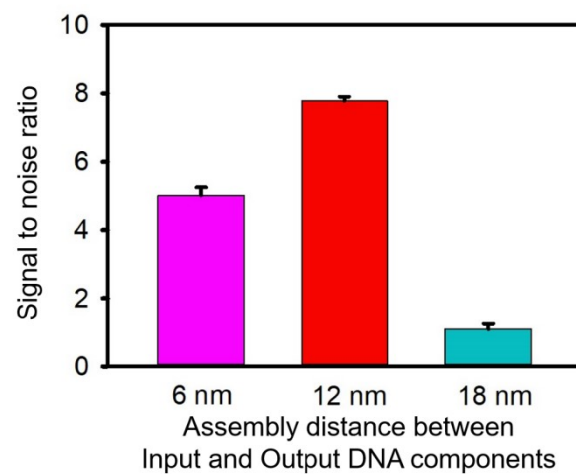


**Figure S8.** The optimizing the assembly distance between input and output DNA components on the AND logic nano-chip. The error bars indicate mean  $\pm$  standard deviation (SD, n = 5). The more detailed descriptions about wiring instructions were given in Figure S44.

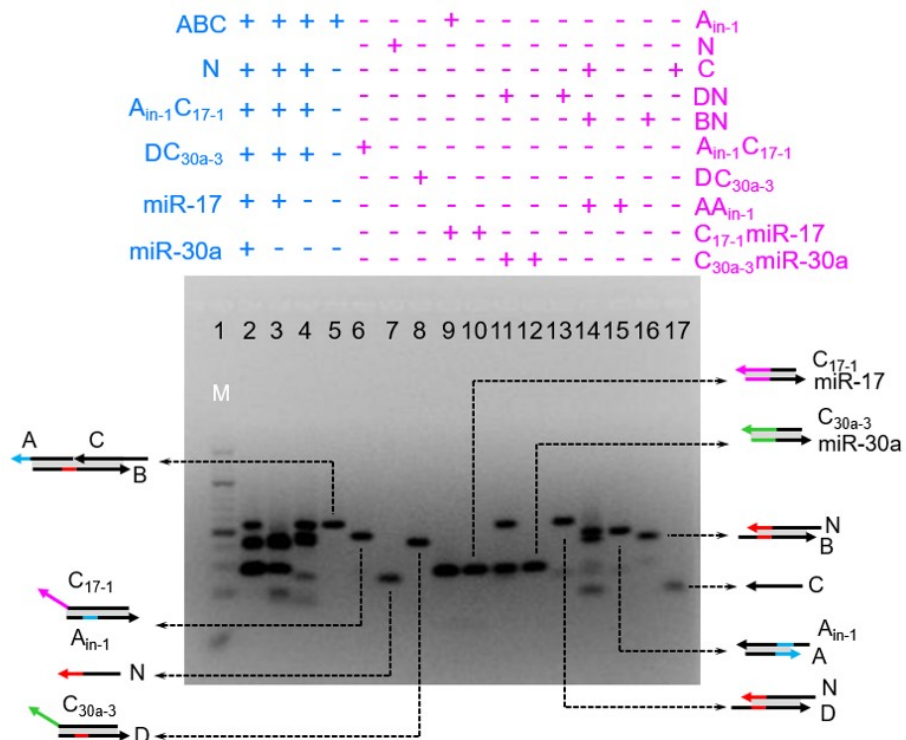


**Figure S9.** Agarose gel electrophoresis analysis of the toehold mediated strand displacement reaction between inputs (miRNA-17 and miRNA-30a) and the functional DNA units, including ssDNA N, two DNA duplex  $A_{in-1}C_{17-1}$ ,  $DC_{30a-3}$  and the triple-stranded complex ABC. Lane 2-5 showed the products of the reactions between inputs and the functional DNA units marked in blue words. Lane 6-17 exhibited the products of the corresponding ssDNA and DNA duplexes marked in purple-red words.

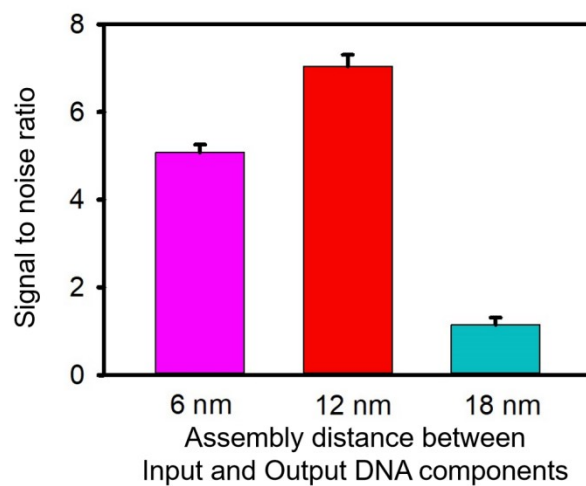


**Figure S10.** The optimizing the assembly distance between input and output DNA components on the AND-NOT logic nano-chip. The error bars indicate mean  $\pm$  standard deviation (SD, n = 5). The more detailed descriptions about wiring instructions were given in Figure S45.

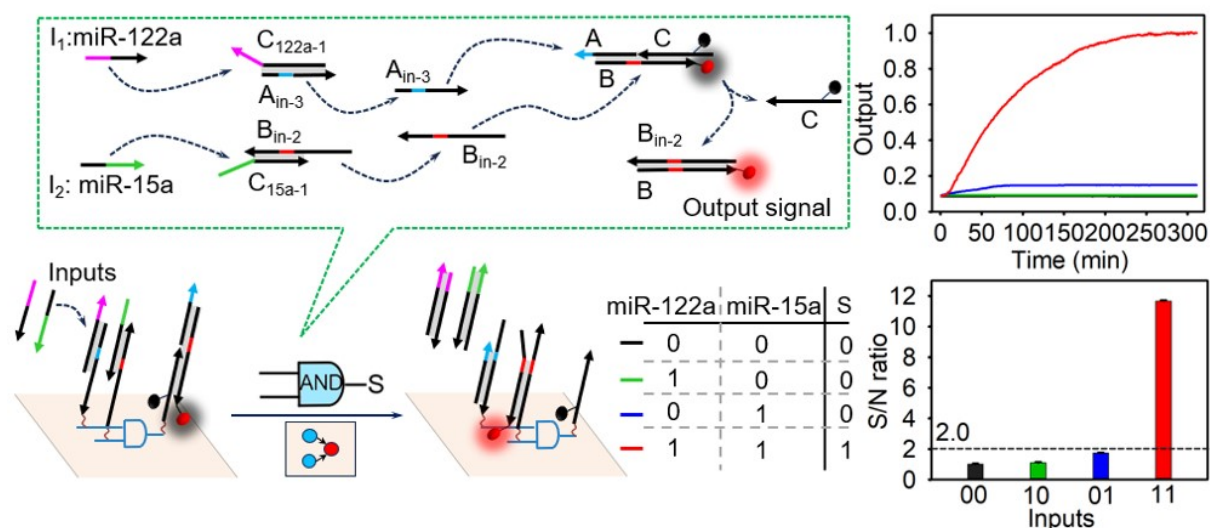


**Figure S11.** Design and performance of the general AND logic nano-chip using two microRNAs (-122a, -15a) as inputs. Brief, two duplex DNA complex  $A_{in-3}C_{122a-1}$ ,  $B_{in-2}C_{15a-1}$  and a triple-stranded DNA complex  $ABC$  were spatially arranged by wiring instruction to form origami-based AND gate. Two duplex DNA complex  $A_{in-3}C_{122a-1}$  and  $B_{in-2}C_{15a-1}$  converted the input microRNAs (-122a and -15a) to single-stranded DNA (ssDNA,  $A_{in-3}$ ,  $B_{in-2}$ ), and the latter hybridized with the triple-stranded DNA complex  $ABC$  to release ssDNA  $C$  and produce new duplex DNA complex  $BB_{in-2}$ , lighting up the fluorescence signal. As expected in the truth value table, when all the two miRNAs were present (1,1), a strong fluorescence signal was obtained with the true/false (1/0) threshold was calculated to be 2.0 and the fluorescence recovery almost reached the maximum after 240 min incubation. The error bars indicate mean  $\pm$  standard deviation (SD,  $n = 5$ ).

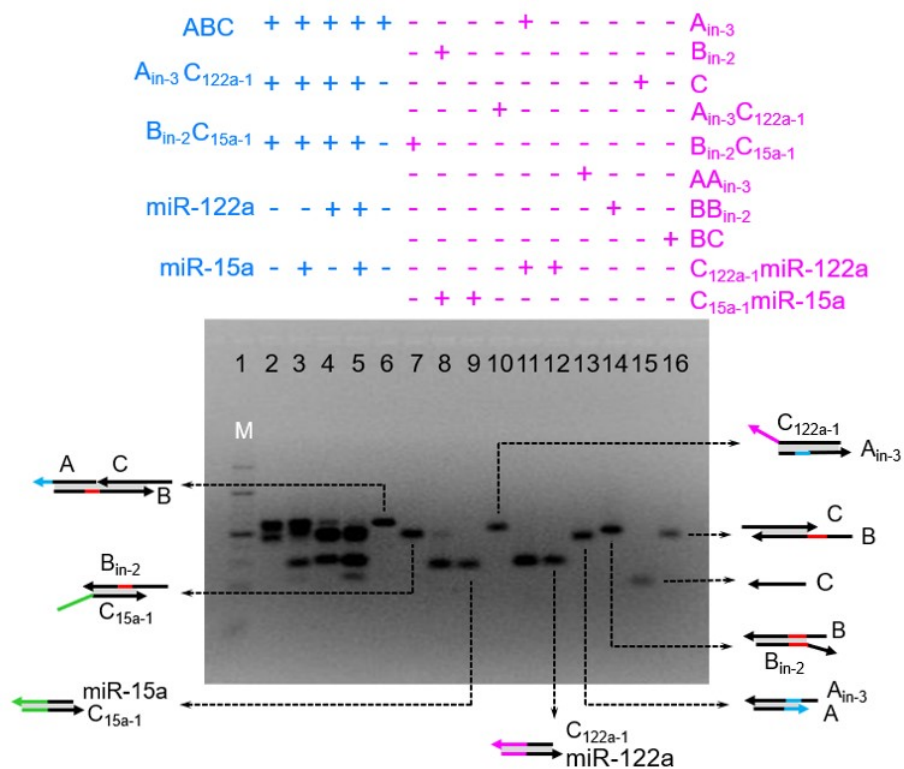


**Figure S12.** Agarose gel electrophoresis analysis of the toehold mediated strand displacement reaction between inputs (miRNA-122a and miRNA-15a) and the functional DNA units, including two DNA duplex  $A_{in-3}C_{122a-1}$ ,  $B_{in-2}C_{15a-1}$  and the triple-stranded complex ABC. Lane 2-6 showed the products of the reactions between inputs and the functional DNA units marked in blue words. Lane 7-16 exhibited the products of the corresponding ssDNA and DNA duplexes marked in purple-red words.

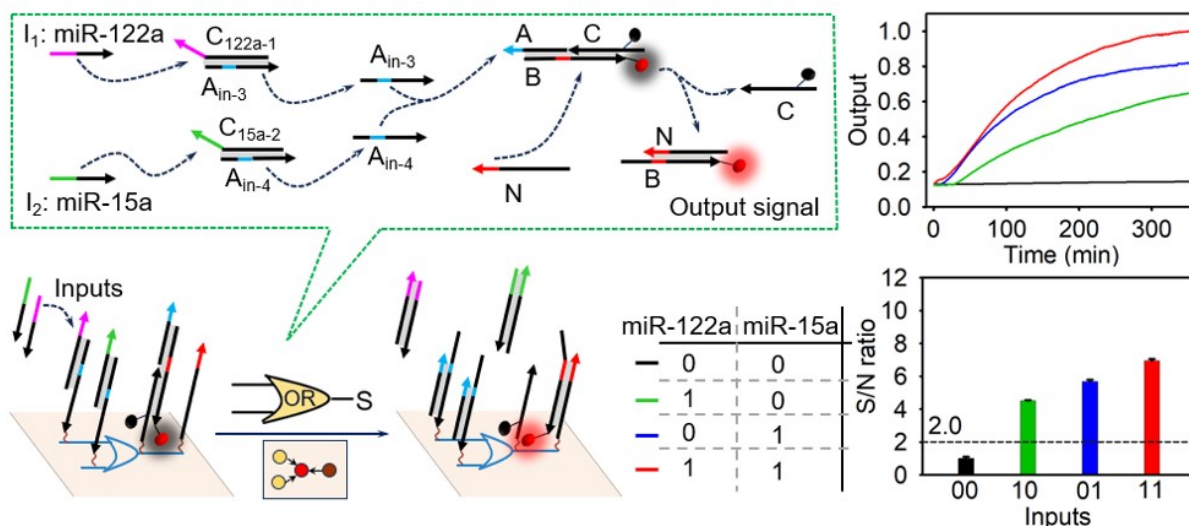


**Figure S13.** Design and performance of the general OR logic nano-chip using two microRNAs (-122a, -15a) as inputs. Brief, one or both two input miRNAs displaced ssDNA A<sub>in-3</sub> or A<sub>in-4</sub> from duplex DNA complex A<sub>in-3</sub>C<sub>122a-1</sub> or A<sub>in-4</sub>C<sub>15a-2</sub>, and the latter hybridized with the triple-stranded DNA complex ABC to release duplex DNA complex BC. Then, ssDNA N liberated ssDNA C and produced duplex DNA complex BN, lighting up the fluorescence signal. As expected in the truth value table, when either one or both inputs were present (0,1), (1,0), (1,1) resulted in significant output fluorescence, and the true/false (1/0) threshold was calculated to be 2.0. The error bars indicate mean ± standard deviation (SD, n = 5).

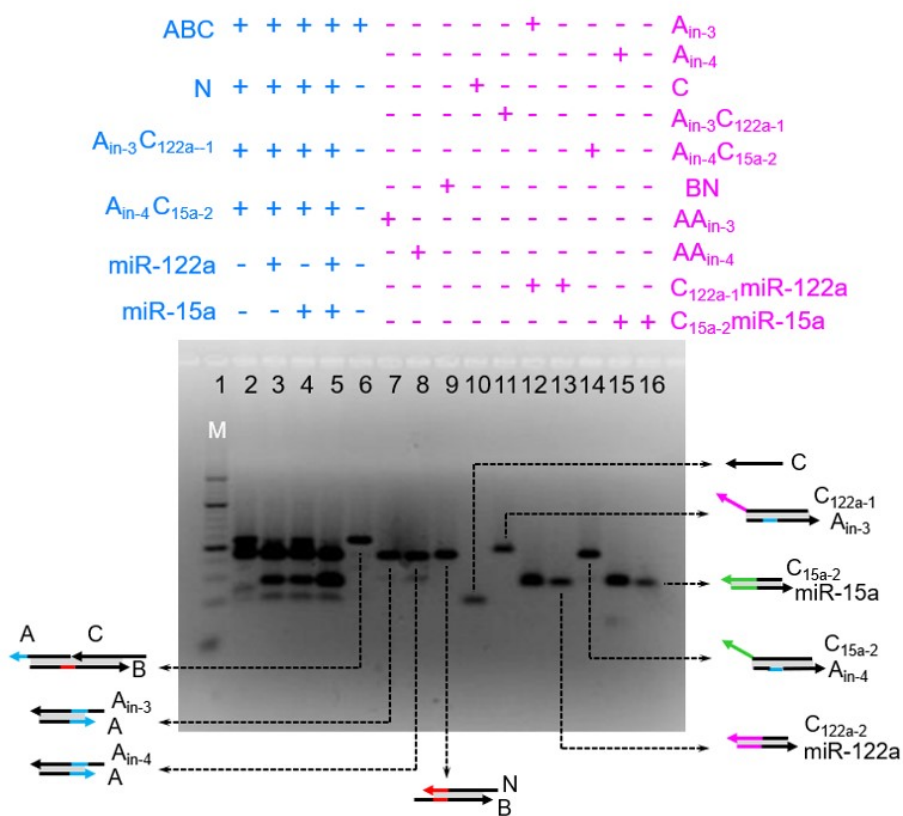


**Figure S14.** Agarose gel electrophoresis analysis of the toehold mediated strand displacement reaction between inputs (miRNA-122a and miRNA-15a) and the functional DNA units, including ssDNA N, two DNA duplex  $A_{in-3}C_{122a-1}$ ,  $A_{in-4}C_{15a-2}$  and the triple-stranded complex ABC. Lane 2-6 showed the products of the reactions between inputs and the functional DNA units marked in blue words. Lane 7-16 exhibited the products of the corresponding ssDNA and DNA duplexes marked in purple-red words.

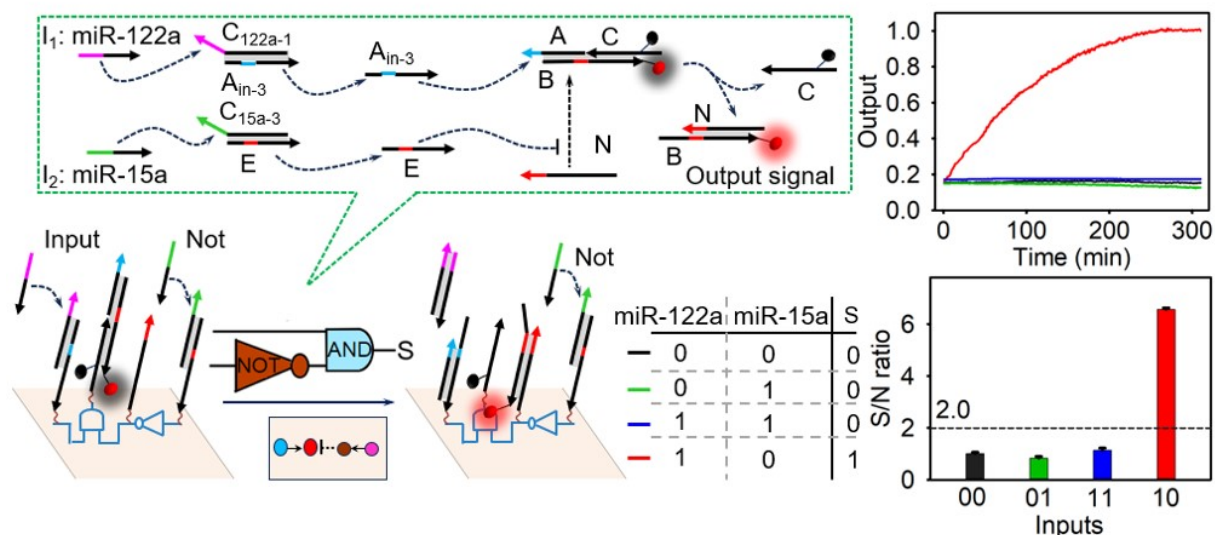


**Figure S15.** Design and performance of the general NOT-AND logic nano-chip using two microRNAs (-122a, -15a) as inputs. Brief, input miRNA-122a displaced ssDNA  $A_{in-3}$  from duplex DNA complex  $A_{in-3}C_{122a-1}$ , and the latter hybridized with the triple-stranded DNA complex  $ABC$  to release duplex DNA complex  $BC$ . In the absence of miRNA-15a, ssDNA  $N$  liberated ssDNA  $C$  and produced duplex DNA complex  $BN$ , lighting up the fluorescence signal. Once in the presence of miRNA-15a, duplex DNA complex  $EC_{15a-3}$  converted it to the ssDNA  $E$ , which could preferentially hybridize with ssDNA  $N$  to prevent subsequent displacement reaction. As expected in the truth value table, the logic cascade nano-chip generated high output signal only in the presence of miRNA-122a and absence of miRNA-15a, and the true/false (1/0) threshold was calculated to be 2.0.

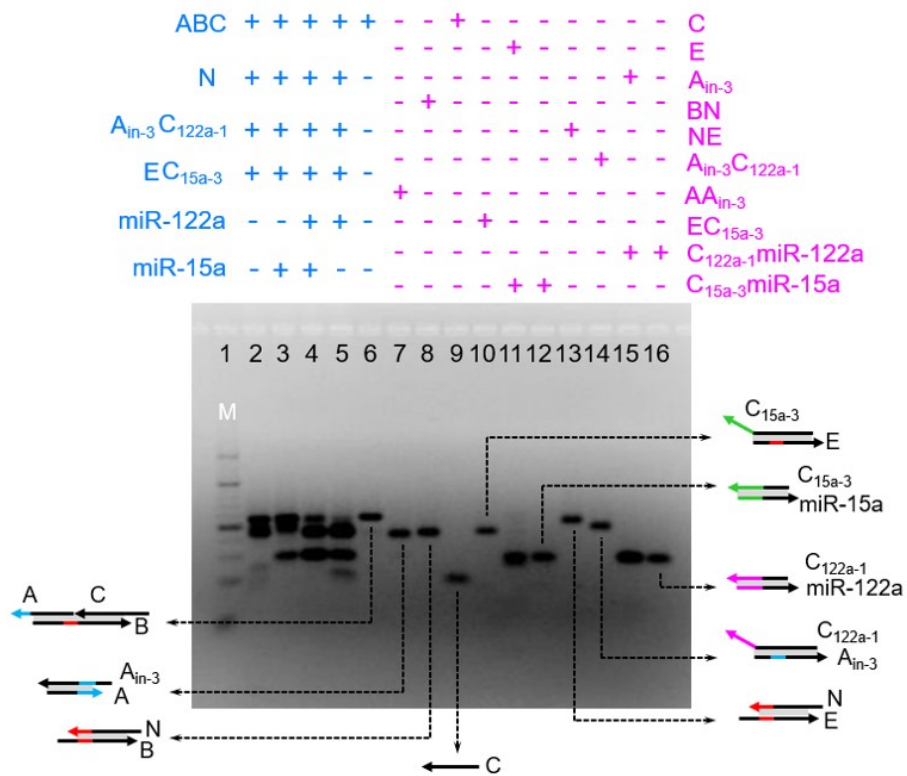


**Figure S16.** Agarose gel electrophoresis analysis of the toehold mediated strand displacement reaction between inputs (miRNA-122a and miRNA-15a) and the functional DNA units, including ssDNA N, two DNA duplex A<sub>in-3</sub>C<sub>122a-1</sub>, EC<sub>15a-3</sub> and the triple-stranded complex ABC. Lane 2-6 showed the products of the reactions between inputs and the functional DNA units marked in blue words. Lane 7-16 exhibited the products of the corresponding ssDNA and DNA duplexes marked in purple-red words.

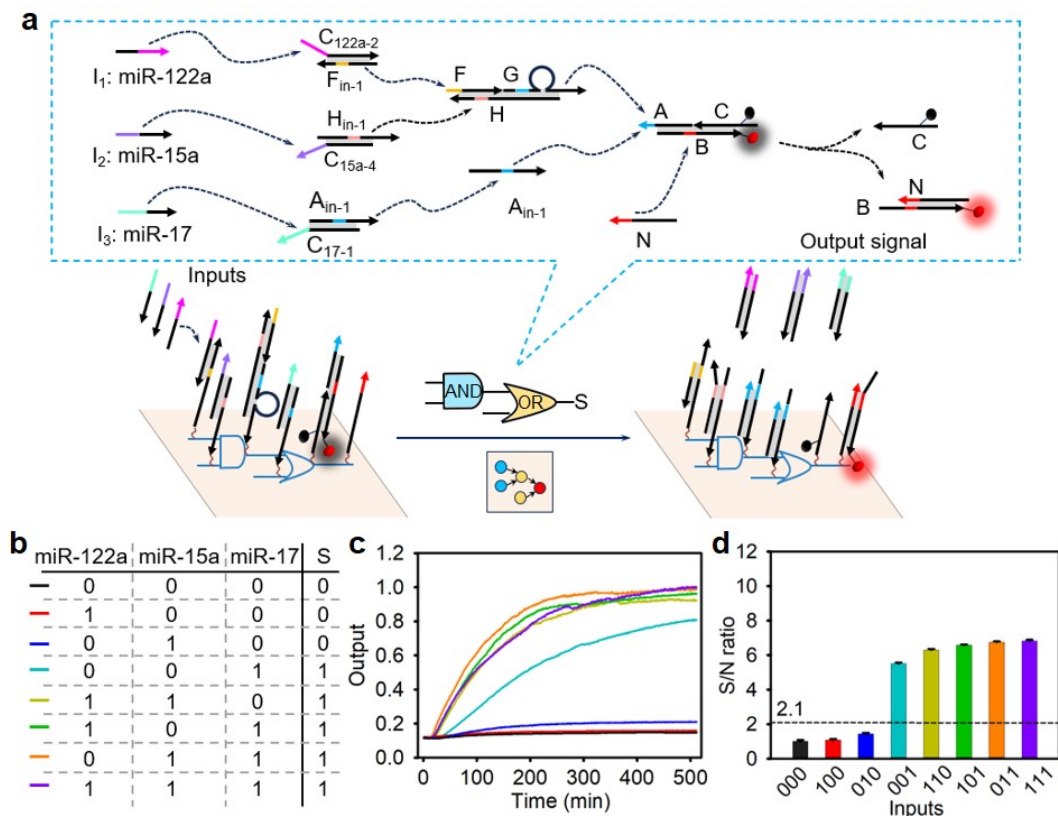


**Figure S17.** Design and performance of the AND-OR logic nano-chip using three microRNAs (-122a, -15a and -17) as inputs. Brief, (a) two duplex DNA complex  $F_{in-1}C_{122a-2}$  and  $H_{in-1}C_{15a-4}$  converted the input microRNAs (-122a and -15a) to single-stranded DNA (ssDNA,  $F_{in-1}$ ,  $H_{in-1}$ ), and the latter hybridized with the triple-stranded DNA complex FGH to release ssDNA G; Input miR-17 displaced ssDNA  $A_{in-1}$  from duplex DNA complex  $A_{in-1}C_{17-1}$ . One of ssDNA G or ssDNA  $A_{in-1}$  could hybridize with the triple-stranded DNA complex ABC to release duplex DNA complex BC. Then, ssDNA N liberated ssDNA C and produced duplex DNA complex BN, lighting up the fluorescence signal. (b) The truth value table of AND-OR logic nano-chip. (c) Time-dependent reactivity of AND-OR logic nano-chip (40 nM) corresponding to different inputs (the concentration of each input miRNAs was 40 nM). (d) S/N ratio obtained from (c) with fluorescence intensity at 300 min. The more detailed descriptions about wiring instructions were given in Figure S42a.

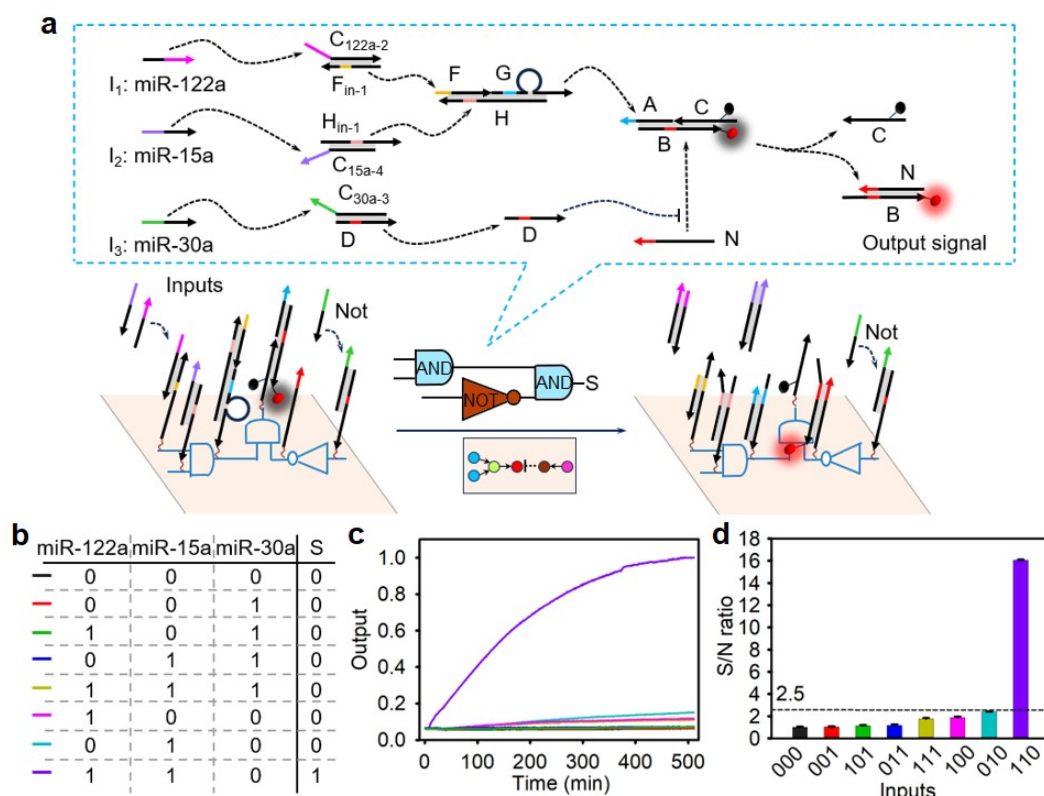


**Figure S18.** Design and performance of the AND-NOT-AND logic nano-chip using three microRNAs (-122a, -15a and -30a) as inputs. Brief, (a) two duplex DNA complex  $F_{in-1}C_{122a-2}$  and  $H_{in-1}C_{15a-4}$  converted the input microRNAs (-122a and -15a) to single-stranded DNA (ssDNA,  $F_{in-1}$ ,  $H_{in-1}$ ), and the latter hybridized with the triple-stranded DNA complex FGH to release ssDNA G. Then the ssDNA G hybridized with the triple-stranded DNA complex ABC to release duplex DNA complex BC. Subsequently, ssDNA N liberated ssDNA C and produced duplex DNA complex BN, lighting up the fluorescence signal. Once in the presence of miRNA-30a, duplex DNA complex  $DC_{30a-3}$  converted it to the ssDNA D, which could preferentially hybridize with ssDNA N to prevent subsequent displacement reaction. (b) The truth value table of AND-NOT-AND logic nano-chip. (c) Time-dependent reactivity of AND-NOT-AND logic nano-chip (40 nM) corresponding to different inputs (the concentration of each input miRNAs was 40 nM). (d) S/N ratio obtained from (c) with fluorescence intensity at 500 min. The more detailed descriptions about wiring instructions were given in Figure S42b.

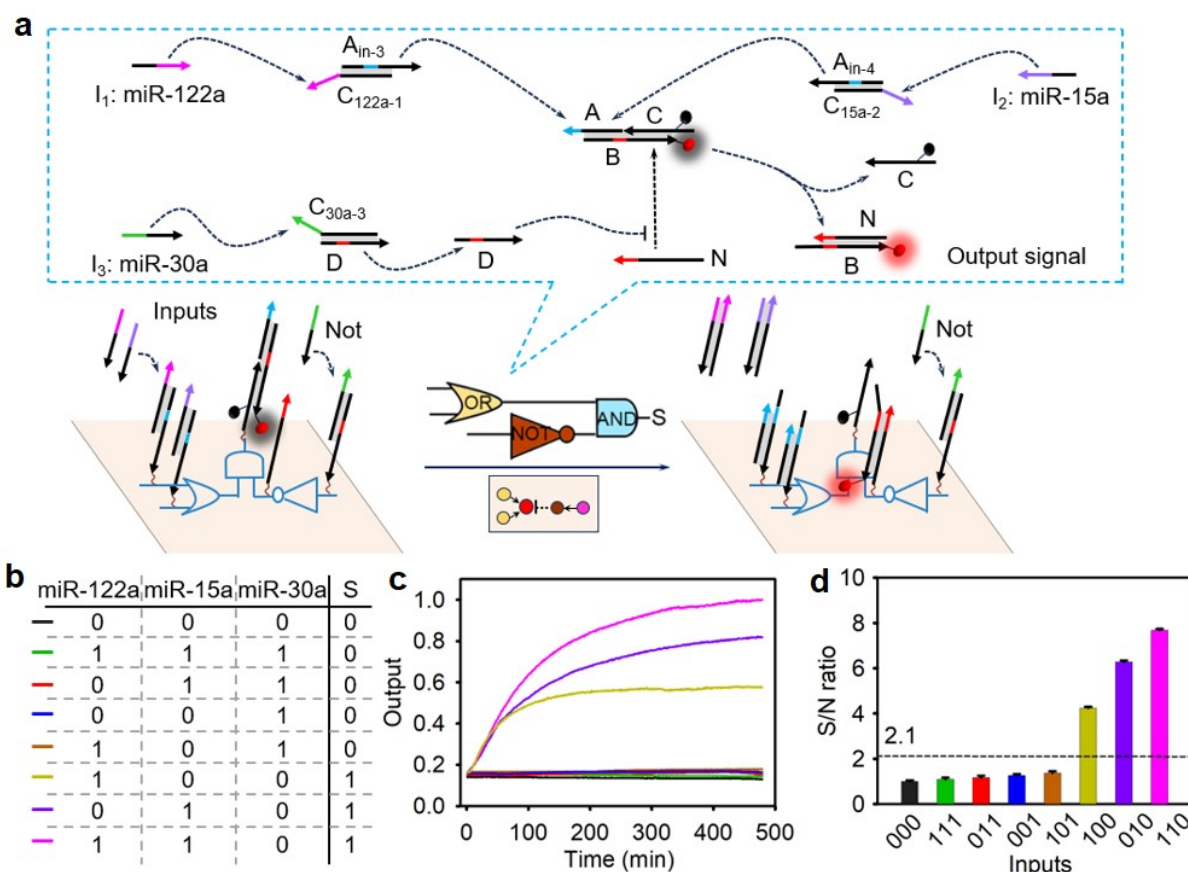


**Figure S19.** Design and performance of the OR-NOT-AND logic nano-chip using three microRNAs (-122a, -15a and -30a) as inputs. Brief, (a) one or both two input miRNAs displaced ssDNA  $A_{in-3}$  or  $A_{in-4}$  from duplex DNA complex  $A_{in-3}C_{122a-1}$  or  $A_{in-4}C_{15a-2}$ , and the latter hybridized with the triple-stranded DNA complex ABC to release duplex DNA complex BC. Then, ssDNA N liberated ssDNA C and produced duplex DNA complex BN, lighting up the fluorescence signal. Once in the presence of miRNA-30a, duplex DNA complex  $DC_{30a-3}$  converted it to the ssDNA D, which could preferentially hybridize with ssDNA N to prevent subsequent displacement reaction. (b) The truth value table of OR-NOT-AND logic nano-chip. (c) Time-dependent reactivity of OR-NOT-AND logic nano-chip (40 nM) corresponding to different inputs (the concentration of each input miRNAs was 40 nM). (d) S/N ratio obtained from (c) with fluorescence intensity at 500 min. The more detailed descriptions about wiring instructions were given in Figure S43a.

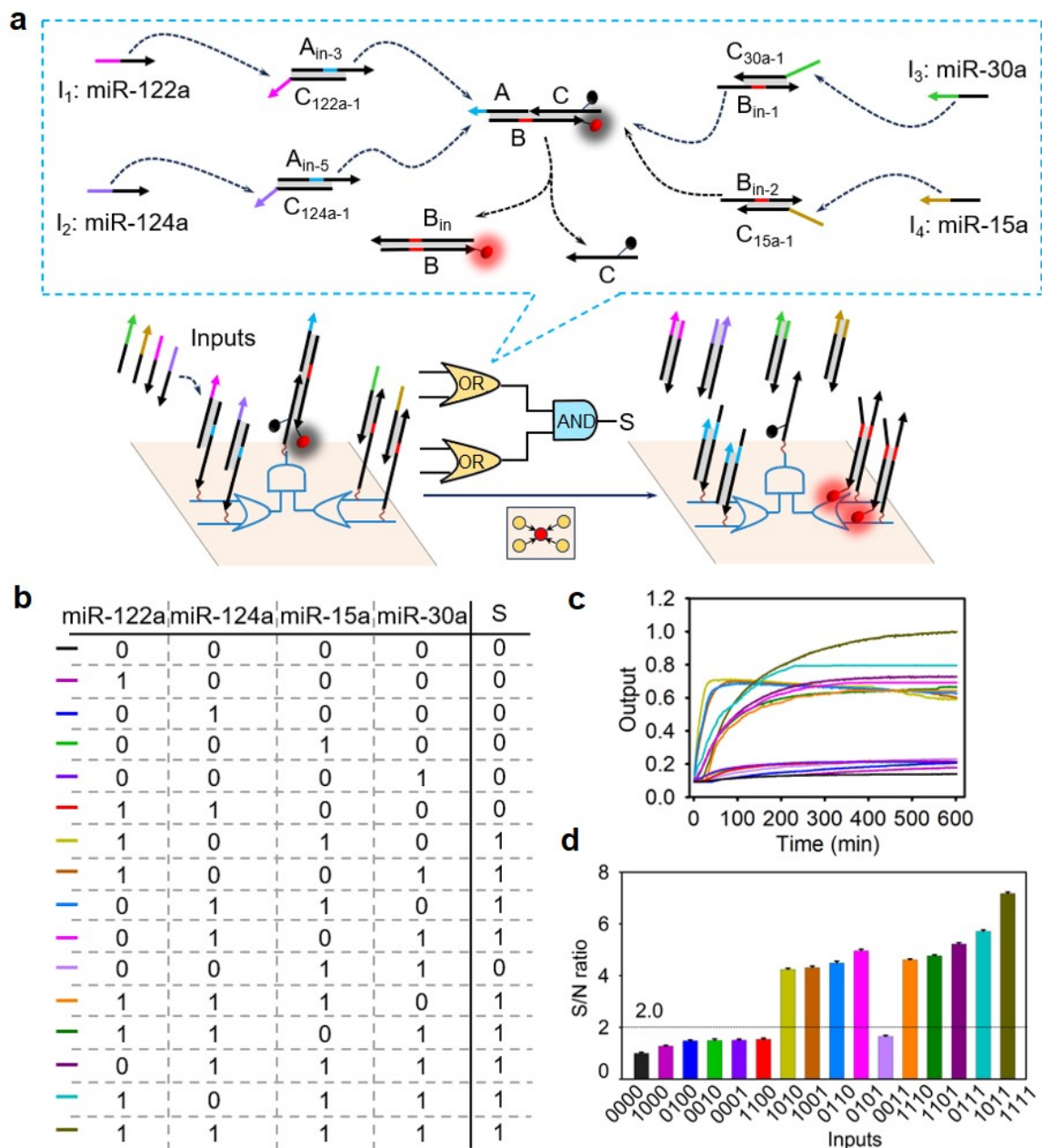


**Figure S20.** Design and performance of the OR-OR-AND logic nano-chip using three microRNAs (-122a, -124a, -15a and -30a) as inputs. Brief, (a) one or both two input miRNAs displaced ssDNA  $A_{in-3}$  or  $A_{in-5}$  from duplex DNA complex  $A_{in-3}C_{122a-1}$  or  $A_{in-5}C_{124a-1}$ , and the latter hybridized with the triple-stranded DNA complex ABC to release duplex DNA complex BC. At the same time, one or both two input miRNAs displaced ssDNA  $B_{in-1}$  or  $B_{in-2}$  from duplex DNA complex  $B_{in-1}C_{30a-1}$  or  $B_{in-2}C_{15a-1}$ , and the latter hybridized with the duplex DNA complex BC to liberate ssDNA C, lighting up the fluorescence signal. (b) The truth value table of OR-OR-AND logic nano-chip. (c) Time-dependent reactivity of OR-OR-AND logic nano-chip (40 nM) corresponding to different inputs (the concentration of each input miRNAs was 40 nM). (d) S/N ratio obtained from (c) with fluorescence intensity at 500 min. The more detailed descriptions about wiring instructions were given in Figure S43b.

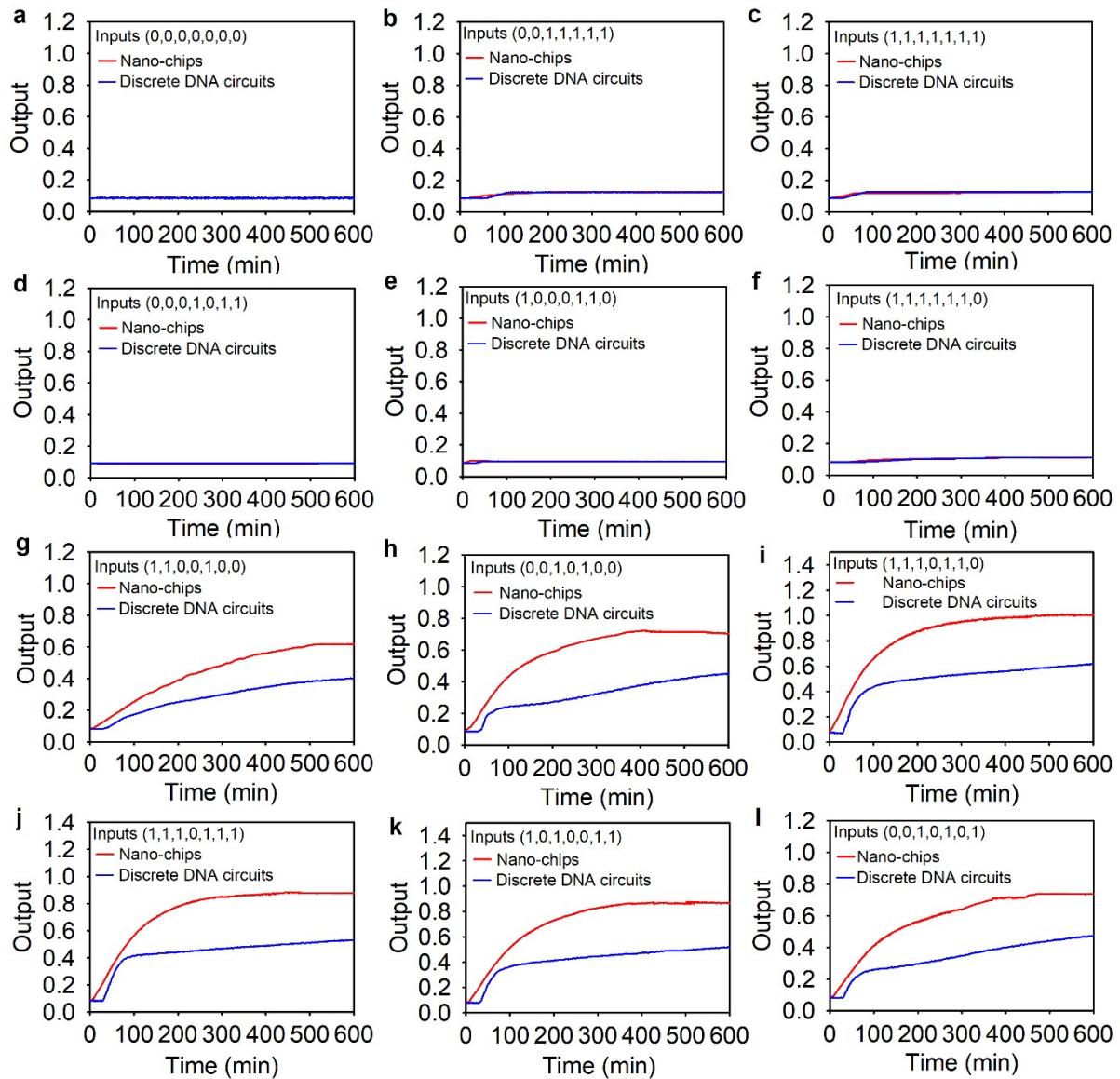


**Figure S21.** Time-dependent Cy5 fluorescence signals (Output  $S_0$ ) of the AND-OR-NOT-AND circuit in nano-chip or discrete DNA circuit response to different inputs (the input order was miR-122a, -15a, -17, -30a, miR-124a, -143 and -10b). (a) The fluorescence signals of Inputs (0, 0, 0, 0, 0, 0, 0); (b) the fluorescence signals of Inputs (0, 0, 1, 1, 1, 1, 1); (c) the fluorescence signals of Inputs (1, 1, 1, 1, 1, 1, 1); (d) the fluorescence signals of Inputs (0, 0, 0, 1, 0, 1, 1); (e) the fluorescence signals of Inputs (1, 0, 0, 0, 1, 1, 0); (f) the fluorescence signals of Inputs (1, 1, 1, 1, 1, 1, 0); (g) the fluorescence signals of Inputs (1, 1, 0, 0, 1, 0, 0), the kinetic rate constant was  $0.0010 \text{ min}^{-1}$  and  $0.0022 \text{ min}^{-1}$  for the diffusible system and nano-chip, respectively; (h) the fluorescence signals of Inputs (0, 0, 1, 0, 1, 0, 0), the kinetic rate constant was  $0.0021 \text{ min}^{-1}$  and  $0.0056 \text{ min}^{-1}$  for the diffusible system and nano-chip, respectively; (i) the fluorescence signals of Inputs (1, 1, 1, 0, 1, 1, 0), the kinetic rate constant was  $0.0043 \text{ min}^{-1}$  and  $0.0166 \text{ min}^{-1}$  for the diffusible system and nano-chip, respectively; (j) the fluorescence signals of Inputs (1, 1, 1, 0, 1, 1, 1), the kinetic rate constant was  $0.0011 \text{ min}^{-1}$  and  $0.0093 \text{ min}^{-1}$  for the diffusible system and nano-chip, respectively; (k) the fluorescence signals of Inputs (1, 0, 1, 0, 0, 1, 1), the kinetic rate constant was  $0.0009 \text{ min}^{-1}$  and  $0.0083 \text{ min}^{-1}$  for the diffusible system and nano-chip, respectively; (l) the fluorescence signals of Inputs (0, 0, 1, 0, 1, 0, 1), the kinetic rate constant was  $0.0009 \text{ min}^{-1}$  and  $0.0050 \text{ min}^{-1}$  for the diffusible system and nano-chip, respectively. Red lines represented the fluorescence signals of nano-chip responded to inputs, blue lines represented the fluorescence signals of discrete DNA circuit responded to inputs.

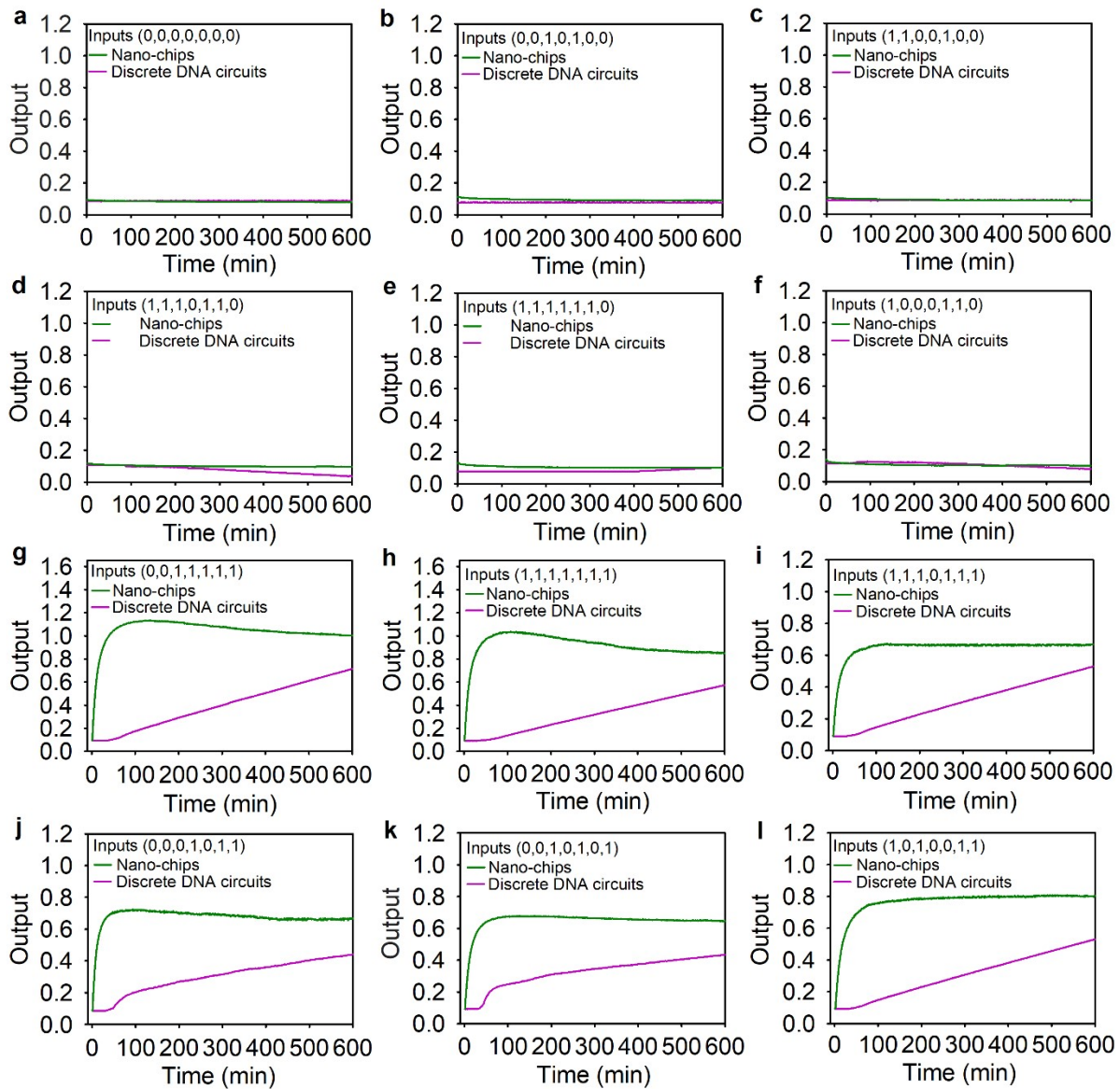


**Figure S22.** Time-dependent FAM fluorescence signals (Output  $S_1$ ) of the OR-AND circuit in nano-chip or discrete DNA circuit response to different inputs (the input order was miR-122a, -15a, -17, -30a, miR-124a, -143 and -10b). (a) The fluorescence signals of Inputs (0, 0, 0, 0, 0, 0, 0); (b) the fluorescence signals of Inputs (0, 0, 1, 0, 1, 0, 0); (c) the fluorescence signals of Inputs (1, 1, 0, 0, 1, 0, 0); (d) the fluorescence signals of Inputs (1, 1, 1, 0, 1, 1, 0); (e) the fluorescence signals of Inputs (1, 1, 1, 1, 1, 1, 0); (f) the fluorescence signals of Inputs (1, 0, 0, 0, 1, 1, 0); (g) the fluorescence signals of Inputs (0, 0, 1, 1, 1, 1, 1), the kinetic rate constant was  $0.0020 \text{ min}^{-1}$  and  $0.0968 \text{ min}^{-1}$  for the diffusable system and nano-chip, respectively; (h) the fluorescence signals of Inputs (1, 1, 1, 1, 1, 1, 1), the kinetic rate constant was  $0.0025 \text{ min}^{-1}$  and  $0.0879 \text{ min}^{-1}$  for the diffusable system and nano-chip, respectively; (i) the fluorescence signals of Inputs (1, 1, 1, 0, 1, 1, 1), the kinetic rate constant was  $0.0013 \text{ min}^{-1}$  and  $0.0303 \text{ min}^{-1}$  for the diffusable system and nano-chip, respectively; (j) the fluorescence signals of Inputs (0, 0, 0, 1, 0, 1, 1), the kinetic rate constant was  $0.0010 \text{ min}^{-1}$  and  $0.0588 \text{ min}^{-1}$  for the diffusable system and nano-chip, respectively; (k) the fluorescence signals of Inputs (0, 0, 1, 0, 1, 0, 1), the kinetic rate constant was  $0.0008 \text{ min}^{-1}$  and  $0.0344 \text{ min}^{-1}$  for the diffusable system and nano-chip, respectively; (l) the fluorescence signals of Inputs (1, 0, 1, 0, 0, 1, 1), the kinetic rate constant was  $0.0013 \text{ min}^{-1}$  and  $0.0383 \text{ min}^{-1}$  for the diffusable system and nano-chip, respectively. Green lines represented the fluorescence signals of nano-chip responded to inputs, purple lines represented the fluorescence signals of discrete DNA circuit responded to inputs.

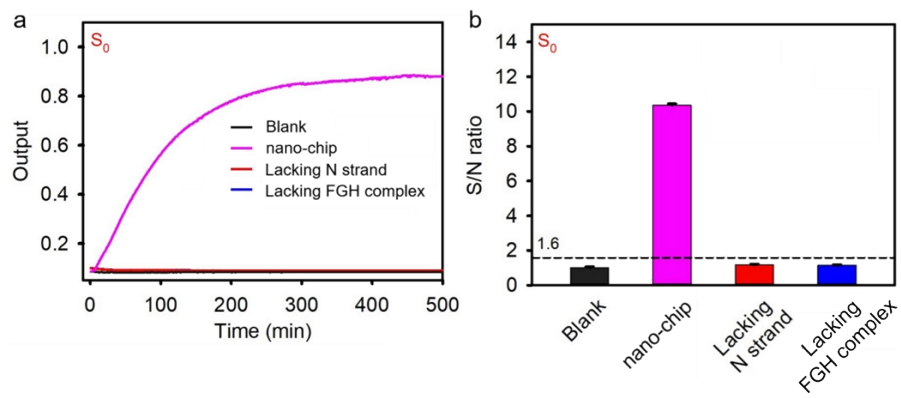


**Figure S23.** The performance of nano-chip loading with AND-OR-NOT-AND circuit and two control nano-chips lacking N strand or the FGh complex in responding to inputs (miR-122a, miR-15a, miR-17).

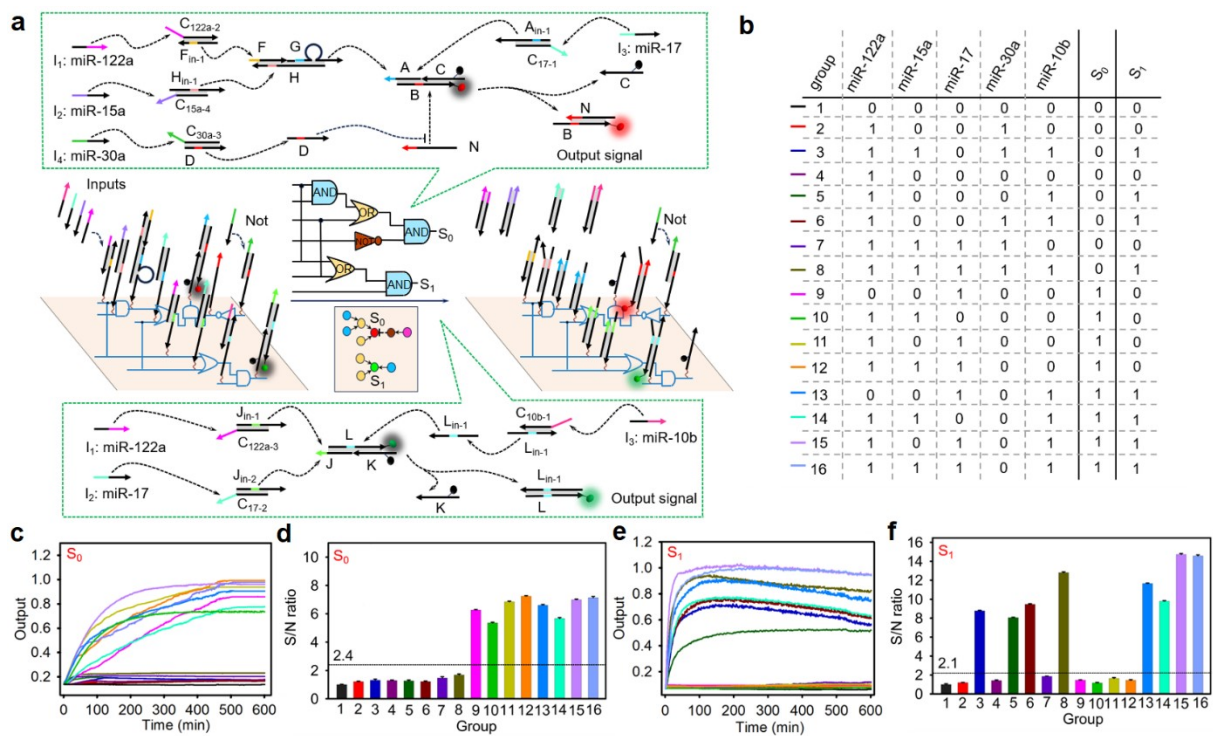


**Figure S24.** Design and performance of the scalable cross-selective nano-chip with 11 addressable dual-rail logical components for five-inputs multi-levels logic cascading and parallel biocomputing. (a) Illustration of its operating mechanism. Brief, in the AND-OR-NOT-AND circuit, two duplex DNA complex  $F_{in-1}C_{122a-2}$  and  $H_{in-1}C_{15a-4}$  converted the input microRNAs (-122a and -15a) to single-stranded DNA (ssDNA,  $F_{in-1}$ ,  $H_{in-1}$ ), and the latter hybridized with the triple-stranded DNA complex FGH to release ssDNA G. Input miR-17 displaced ssDNA  $A_{in-1}$  from duplex DNA complex  $A_{in-1}C_{17-1}$ . One of ssDNA G or ssDNA  $A_{in-1}$  hybridized with the triple-stranded DNA complex ABC to release duplex DNA complex BC. Then, ssDNA N liberated ssDNA C and produced duplex DNA complex BN, lighting up the fluorescence signal  $S_0$ . Once in the presence of miR-30a, duplex DNA complex  $DC_{30a-3}$  converted it to the ssDNA D, which could preferentially hybridize with ssDNA N to prevent subsequent displacement reaction. In the OR-AND circuit, one or both two input miRNAs displaced ssDNA  $J_{in-1}$  or  $J_{in-2}$  from duplex DNA complex  $J_{in-1}C_{122a-3}$  or  $J_{in-2}C_{17-2}$ , and the latter hybridized with the triple-stranded DNA complex JKL to release duplex DNA complex KL. Input miR-10b displaced ssDNA  $L_{in-1}$  from duplex DNA complex  $L_{in-1}C_{10b-1}$ . Then, ssDNA  $L_{in-1}$  liberated ssDNA K and produced duplex DNA complex  $LL_{in-1}$ , lighting up the fluorescence signal  $S_1$ . The top view of the localized circuit on origami showed the three basic logic gates as color-coded circles (AND: blue; OR: Yellow; NOT: brown; the assistant component of NOT gate: purple red; output  $S_0$ : red; output  $S_1$ : green). The segments with same color are complementary sequences of toehold domain. The more detailed descriptions about wiring instructions were given in Figure S44b. (b) The truth value table of the parallel nano-chip; (c) time-dependent reactivity of AND-OR-NOT-AND circuit corresponding to different inputs; (d) S/N ratio obtained from (c) with fluorescence intensity at 500 min; (e) time-dependent reactivity of OR-AND circuit corresponding to different inputs; (f) S/N ratio obtained from (e) with fluorescence intensity at 200 min.



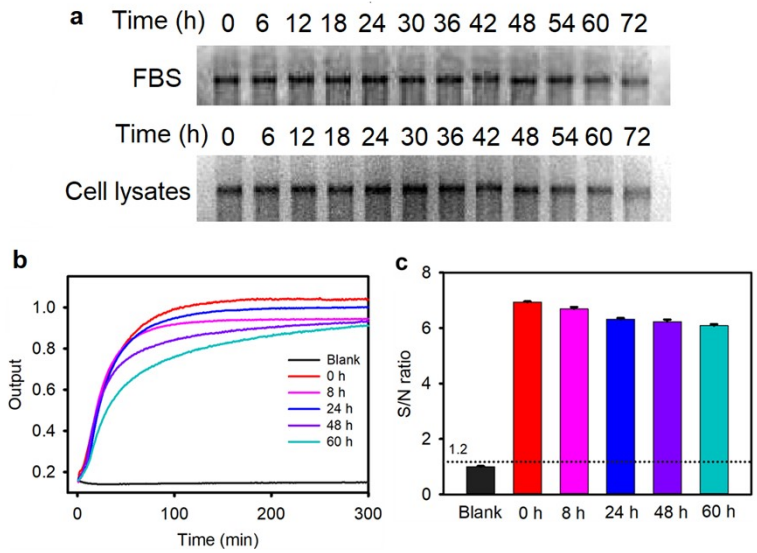


**Figure S26.** Study on the stability of the nano-chip. (a) Degradation analysis of nano-chip in DMEM medium containing 10% FBS (up) and cell lysates (down) at 37°C for different times. (b) the real-time kinetic monitoring of nano-chip (integrated with a three-input AND logic circuit) in responding to inputs (miR-21, miR-17 and miR-30a), the nano-chip was pre-incubated with cell lysates for different times (0, 8, 24, 48 and 60 h). (c) S/N ratio obtained from (b) with fluorescence intensity at 200 min.

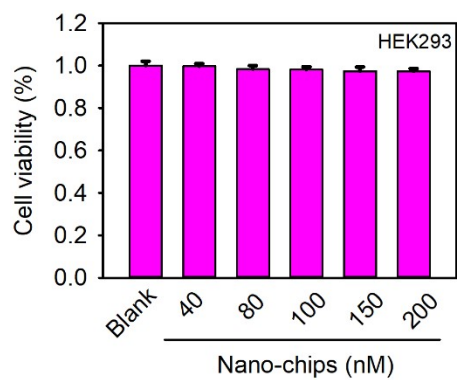


**Figure S27.** Cell viability of HEK293 cells after incubated with different concentrations of nano-chip (0, 40, 80, 100, 150 and 200 nM) at 37°C for 48 h.

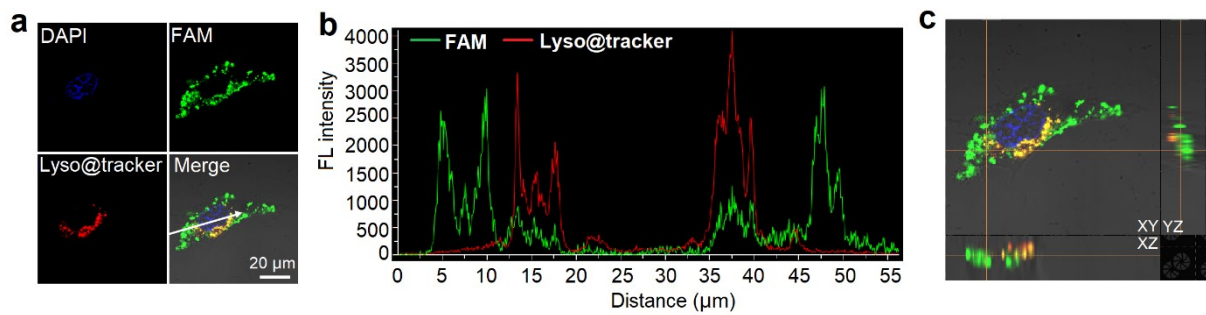


**Figure S28.** Endo-lysosomal release of nano-chip in HeLa cells. (a) CLSM images of HeLa cells after incubation with 40 nM FAM-modified nano-chip for 4 h followed by staining with 75 nM Lyso@Tracker Red and 10 μg/mL Hoechst 33342 for 25 min, scale bar: 20 μm. (b) The fluorescence intensity curves of Lyso@Tracker and FAM in the regions marked straight white line of (a). (c) Confocal z-stacks images with a cross-section in xy, xz and yz for localization of nano-chip in HeLa cells.

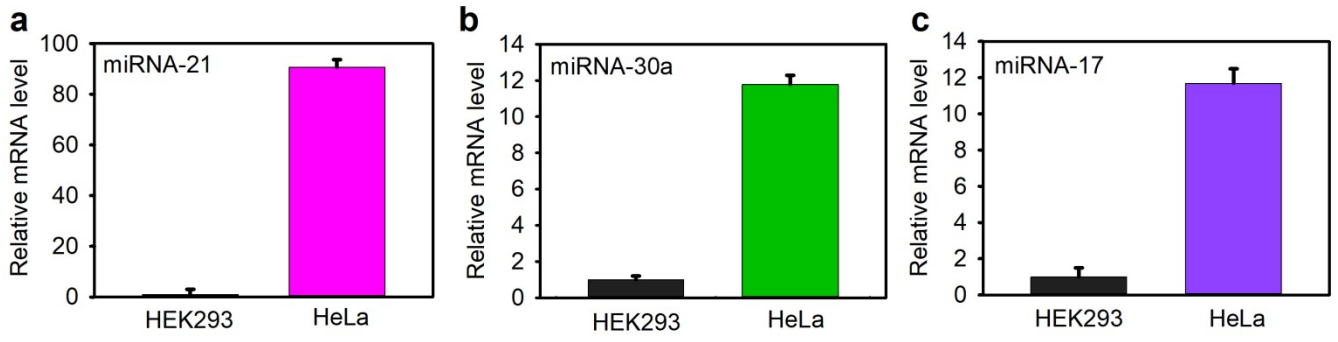


**Figure S29.** The relative expression levels of miRNAs in HEK293 and HeLa cells by using quantitative reverse transcription-PCR (qRT-PCR) analysis method. (a) miRNA-21, (b) miRNA-30a and (c) miRNA-17.

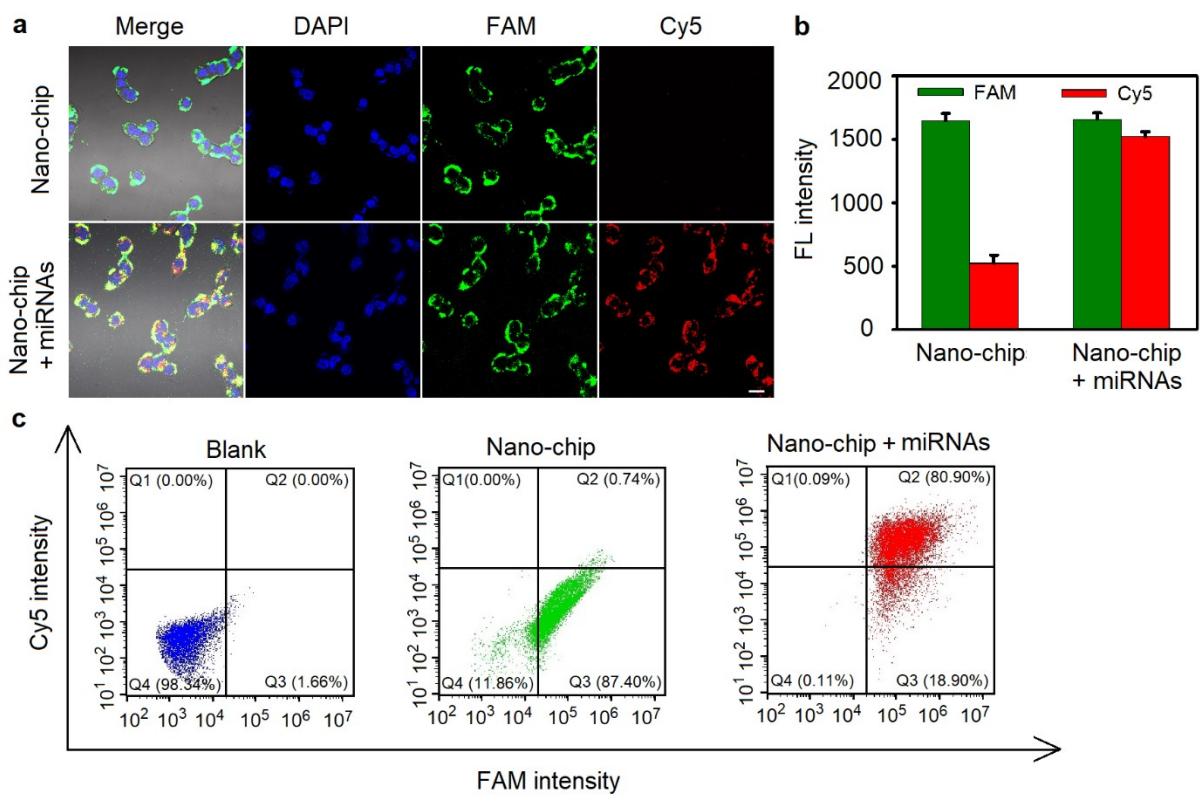


**Figure S30.** The performance of nano-chip in HEK293 cell. (a) CLSM images of HEK293 cells after different treatments, scale bar: 20  $\mu\text{m}$ . (b) The relevant statistical histogram analysis of the CLSM images. (c) The corresponding flow cytometry analysis for HEK293 cells after different treatments.

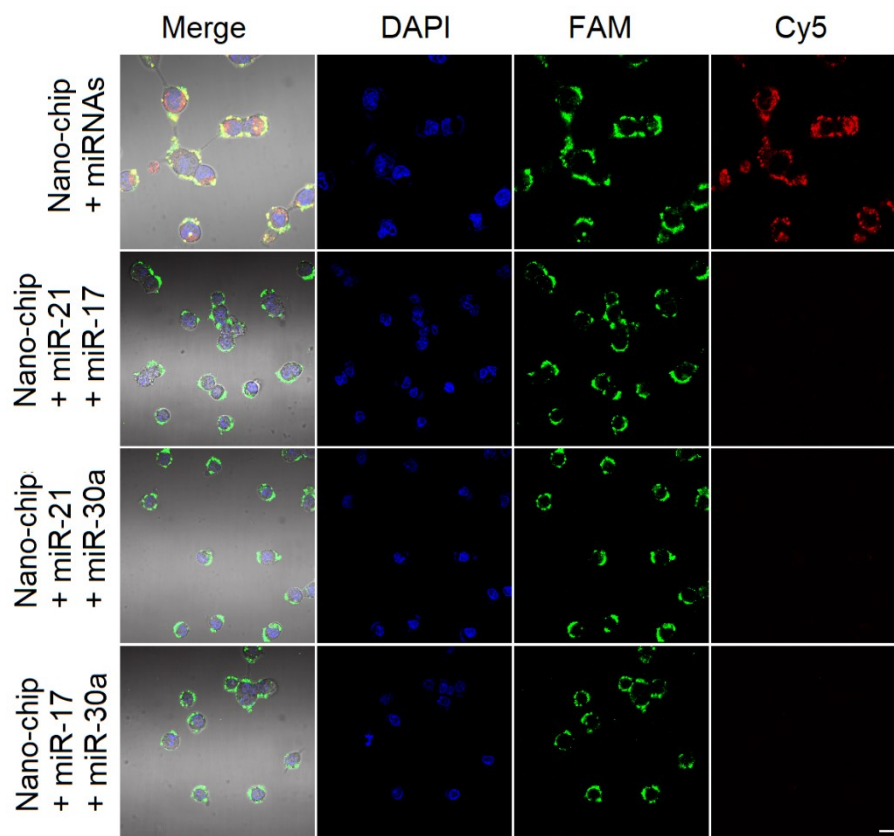


**Figure S31.** CLSM images of HEK293 cells after pre-treated with different miRNA mimics following incubation with nano-chip, scale bar: 20  $\mu$ m.

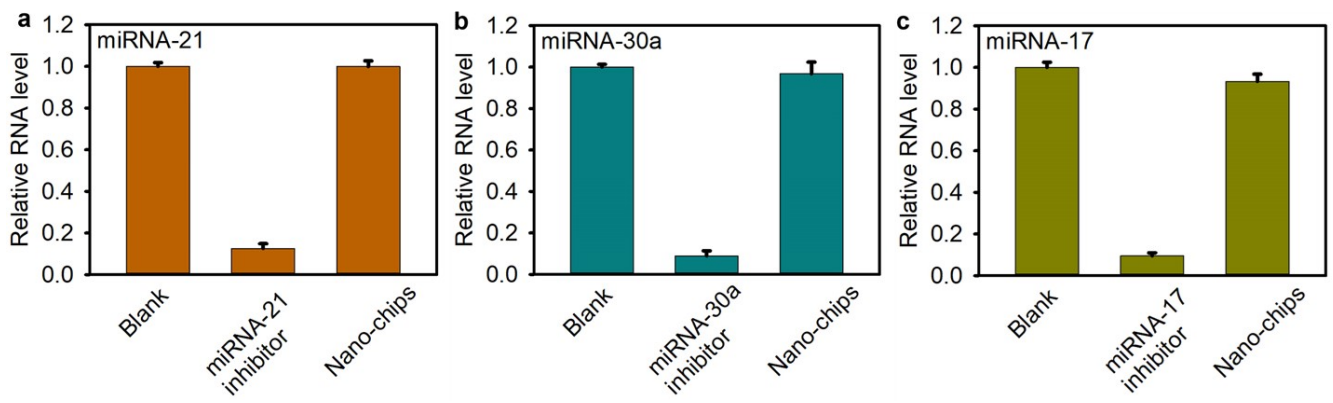


**Figure S32.** The relative expression levels of miRNAs in HeLa cells after treated with different miRNA inhibitors. (a) miRNA-21, (b) miRNA-30a and (c) miRNA-17.

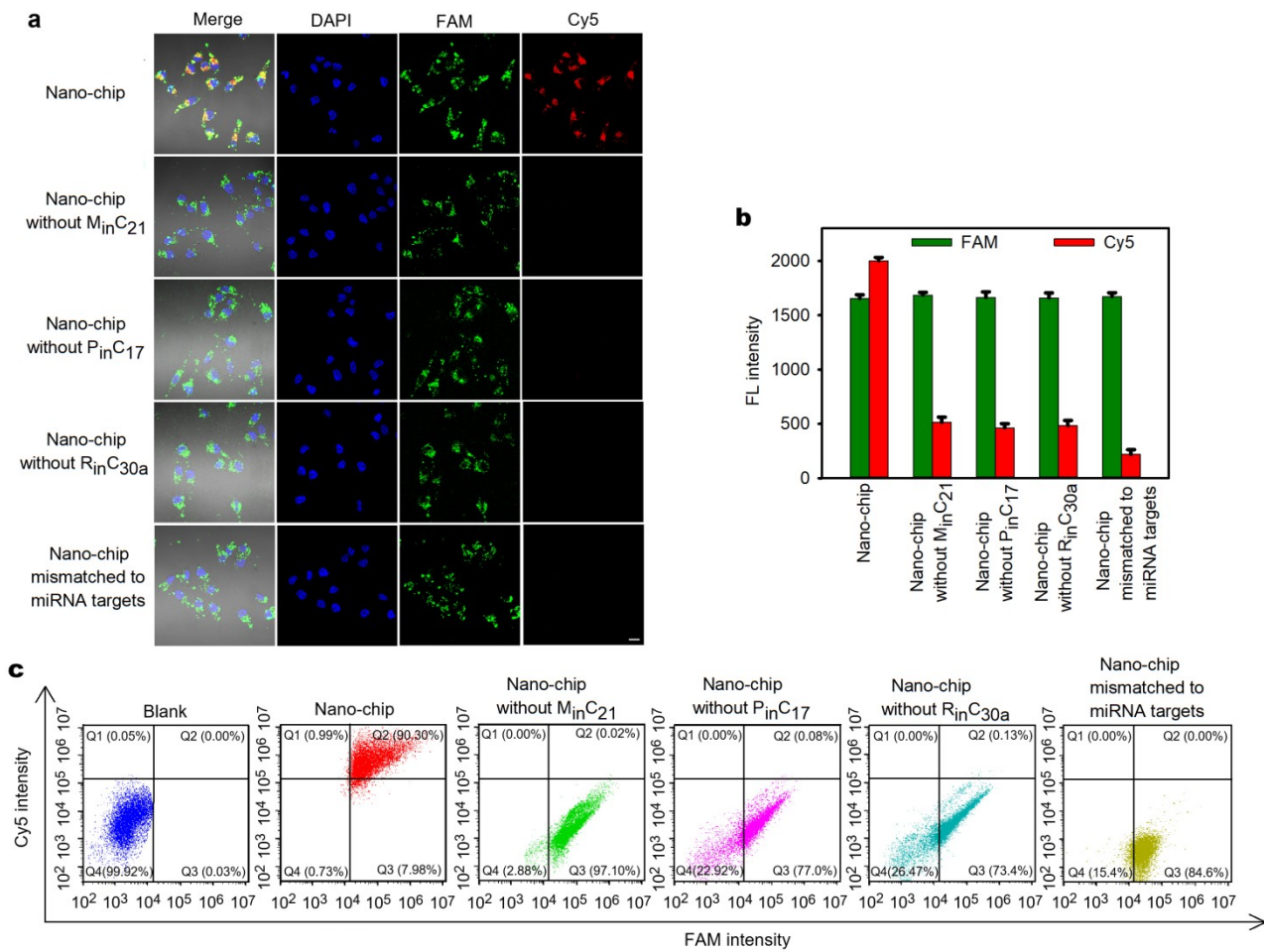


**Figure S33.** The performance of different nano-chips in Hela cell. (a) CLSM images of Hela cells after incubated with different nano-chips, scale bar: 20  $\mu\text{m}$ . (b) The relevant statistical histogram analysis of the CLSM images. (c) The corresponding flow cytometry analysis for Hela cells after different treatments. In the Nano-chip mismatched to miRNA targets, this mismatched control nano-chip was designed to have the same structural configuration as the fully complementary AND logic gate, but with 2 base pair mismatches in the miRNA toehold-recognized regions.

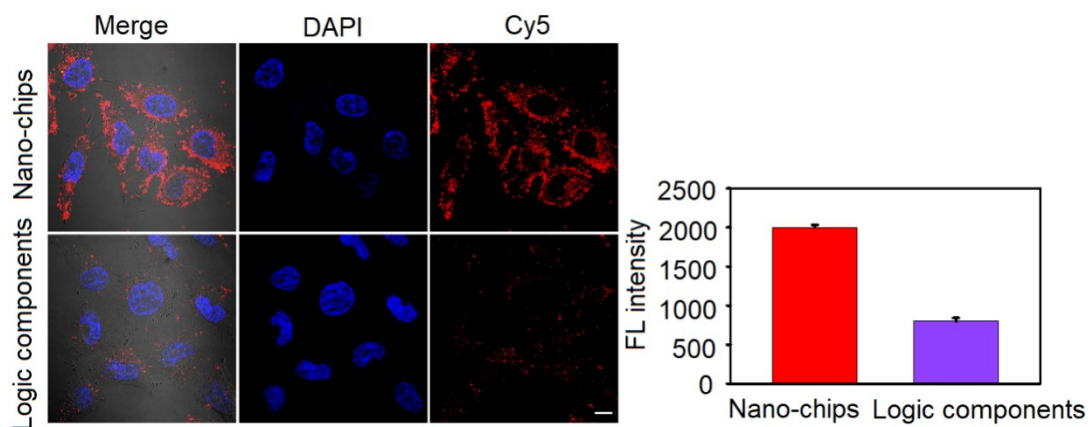


**Figure S34.** (a) CLSM images of HeLa cells after different treatments. Up: nano-chip. Down: discrete DNA logic components, scale bar: 20  $\mu\text{m}$ . (b) The relevant statistical histogram analysis of the CLSM images.

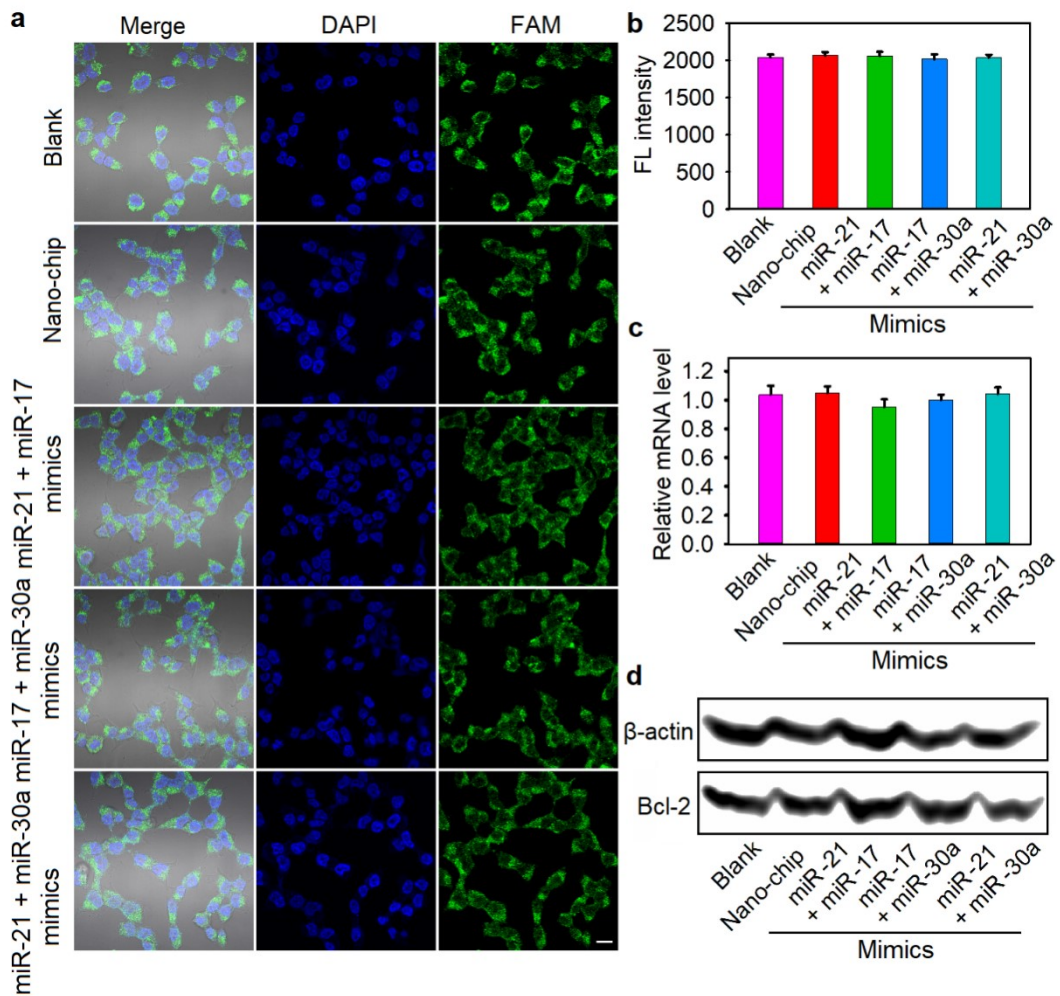


**Figure S35.** (a) Immuno-fluorescence imaging of Bcl2 protein in HEK293 cells after different treatments, scale bar: 20  $\mu$ m. (b) The relevant statistical histogram analysis of the Immuno-fluorescence imaging. (c) The relative expression levels of Bcl2 mRNA in HEK293 cells after different treatments. (d) Western blotting assay of Bcl2 protein from cell lysate from HEK293 cells after different treatments.

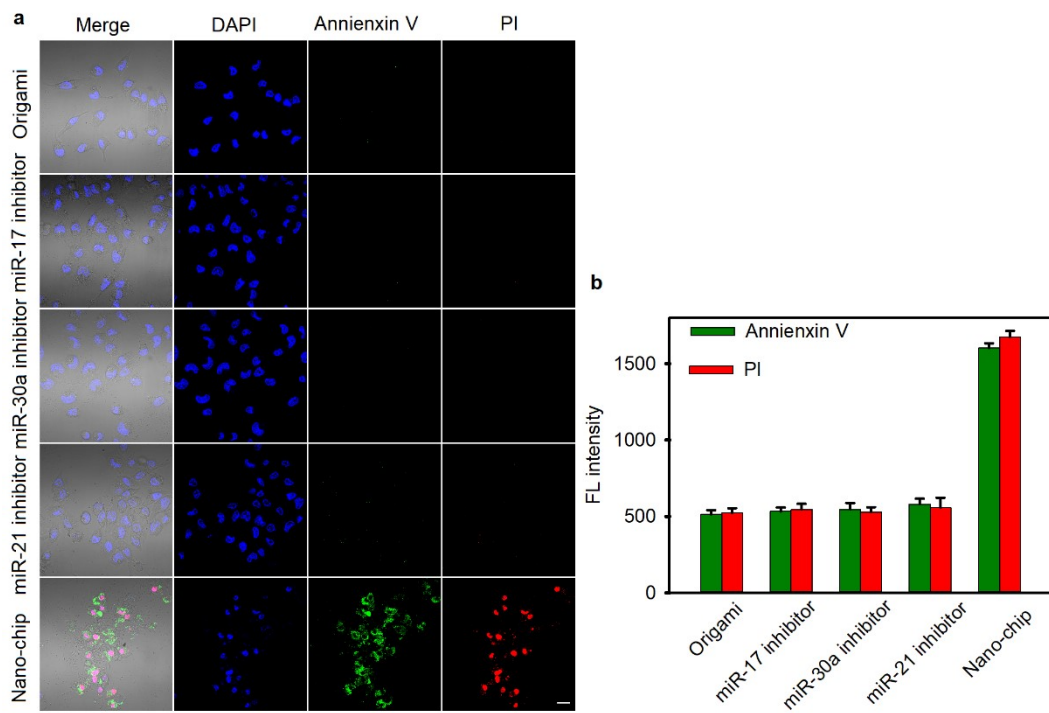


**Figure S36.** (a) The CLSM images of HeLa cells after different treatments by using Annexin V and the PI dead cell apoptosis kit, scale bar: 20  $\mu$ m. (b) The relevant statistical histogram analysis of the CLSM images.

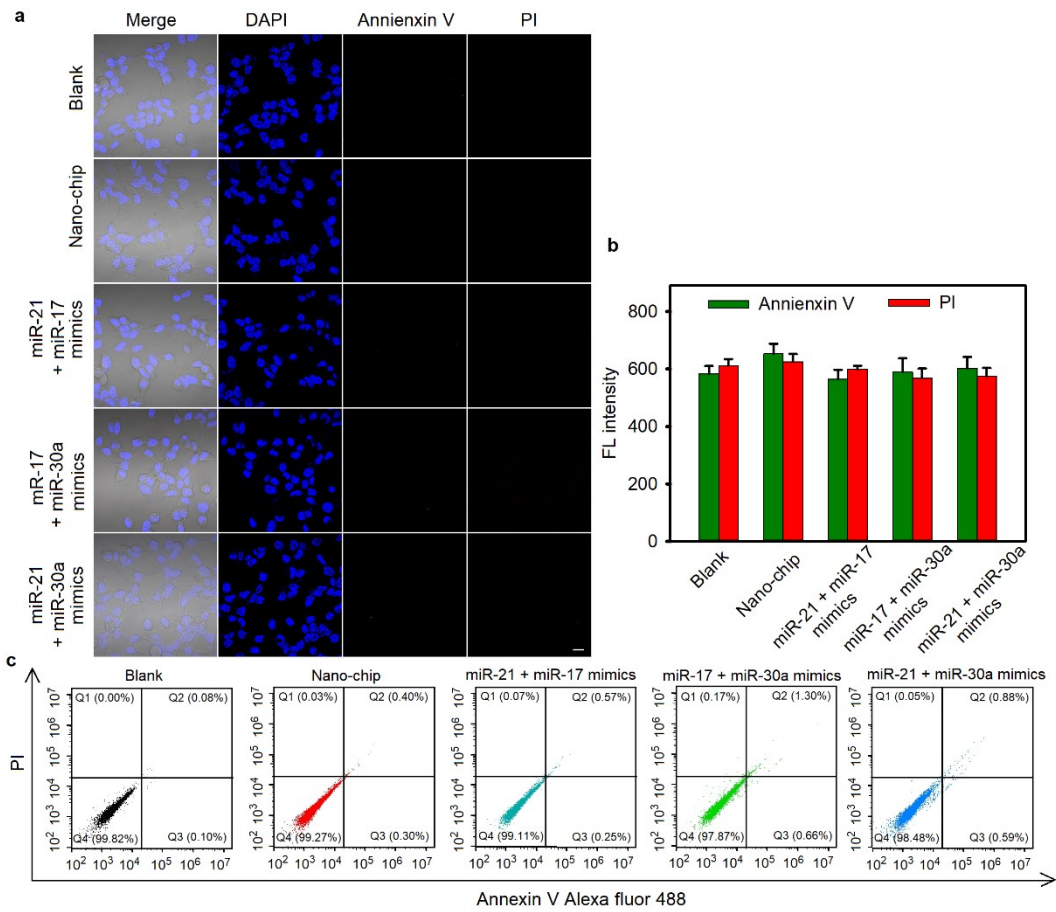


**Figure S37.** (a) The CLSM images of HEK293 cells after different treatments by using Annexin V and the PI dead cell apoptosis kit, scale bar: 20  $\mu\text{m}$ . (b) The relevant statistical histogram analysis of the CLSM images. (c) Flow cytometry assay of analyzing apoptosis in HEK293 cells after different treatments by using Annexin V and the PI dead cell apoptosis kit.

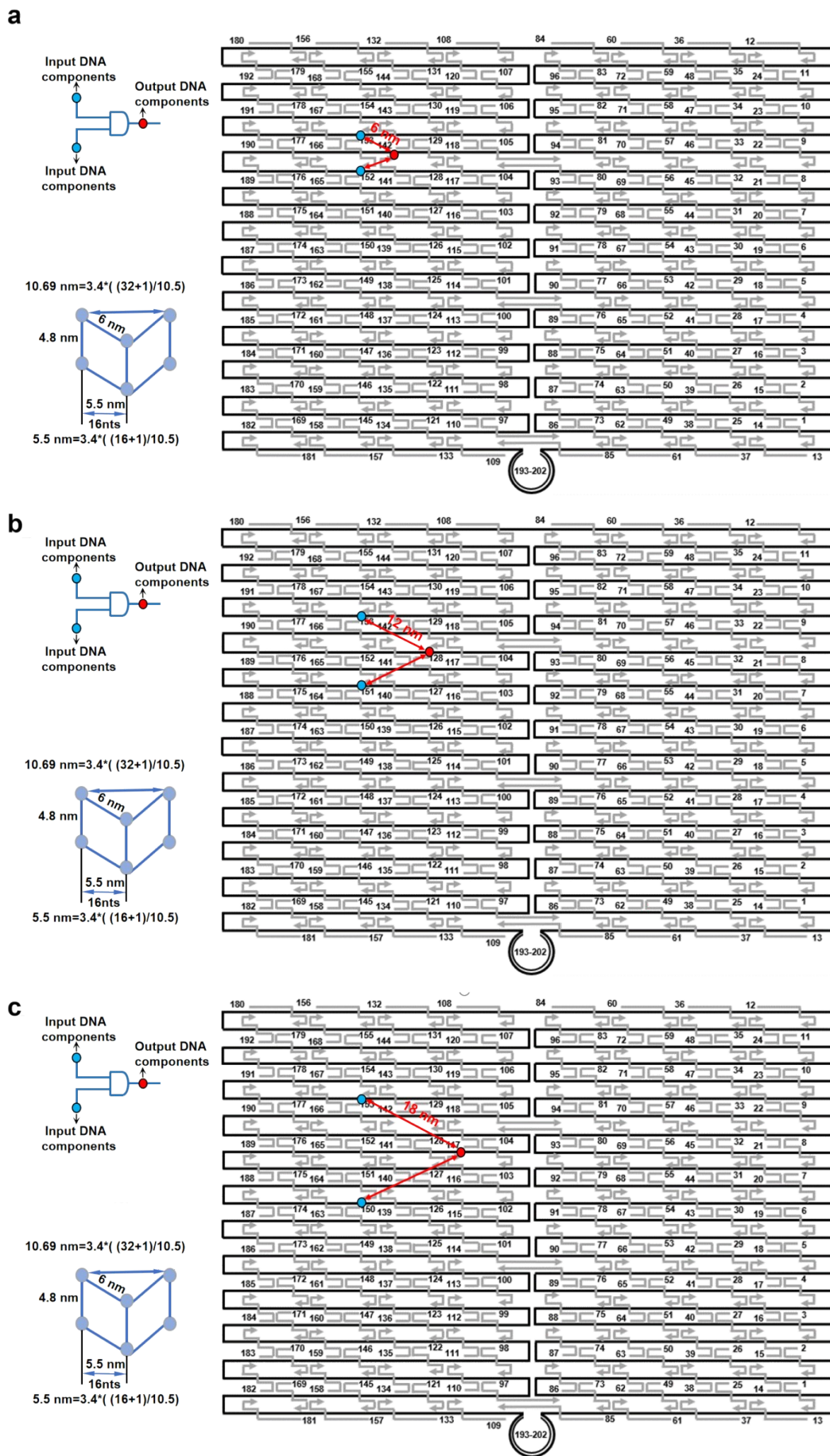


**Figure S38.** The wiring instructions of the AND logic gate with different assembly distance between Input and Output DNA components on DNA origami. (a) 6 nm; (b) 12 nm; (c) 18 nm.

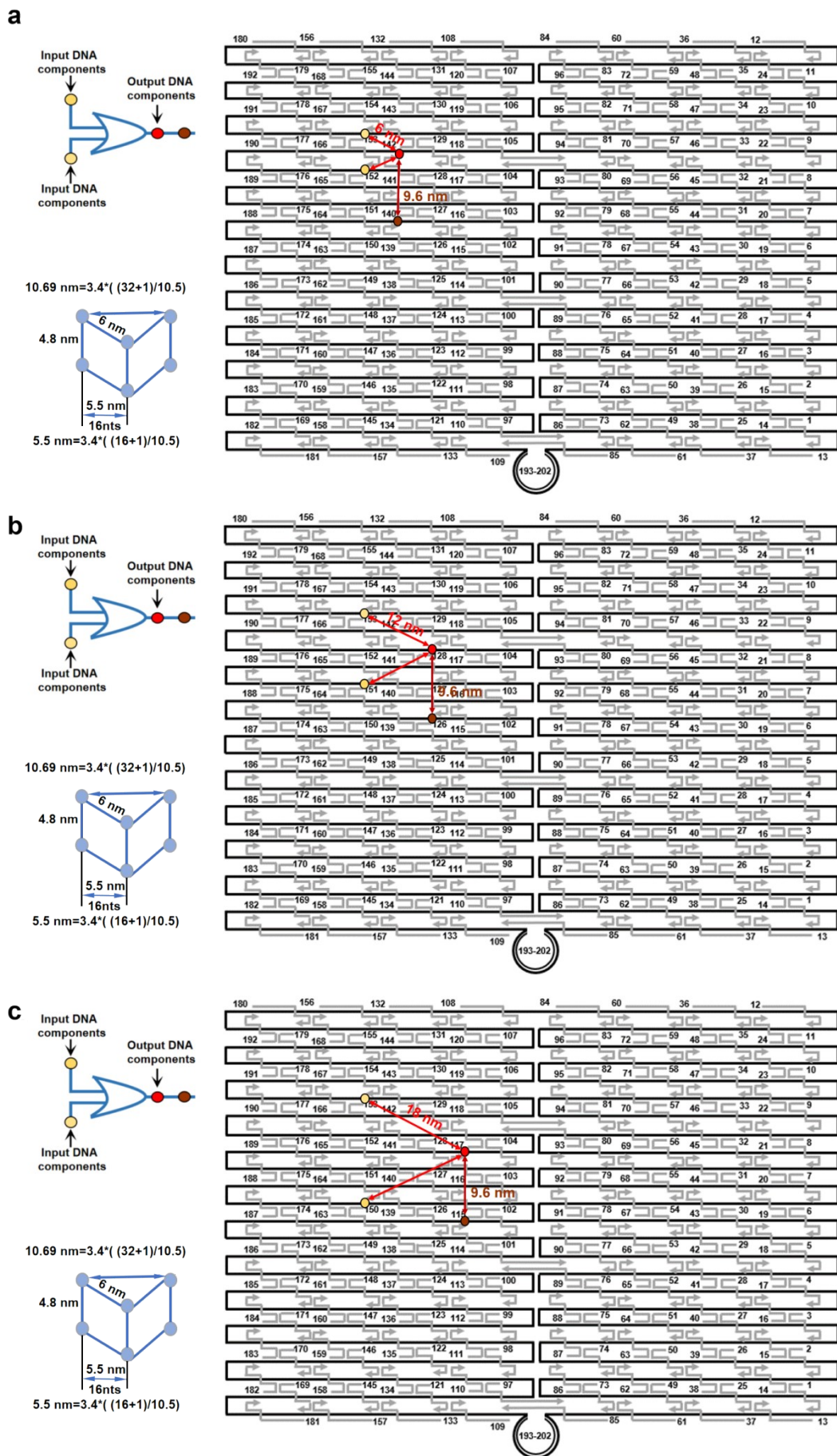


**Figure S39.** The wiring instructions of the OR logic gate with different assembly distance between Input and Output DNA components on DNA origami. (a) 6 nm; (b) 12 nm; (c) 18 nm.

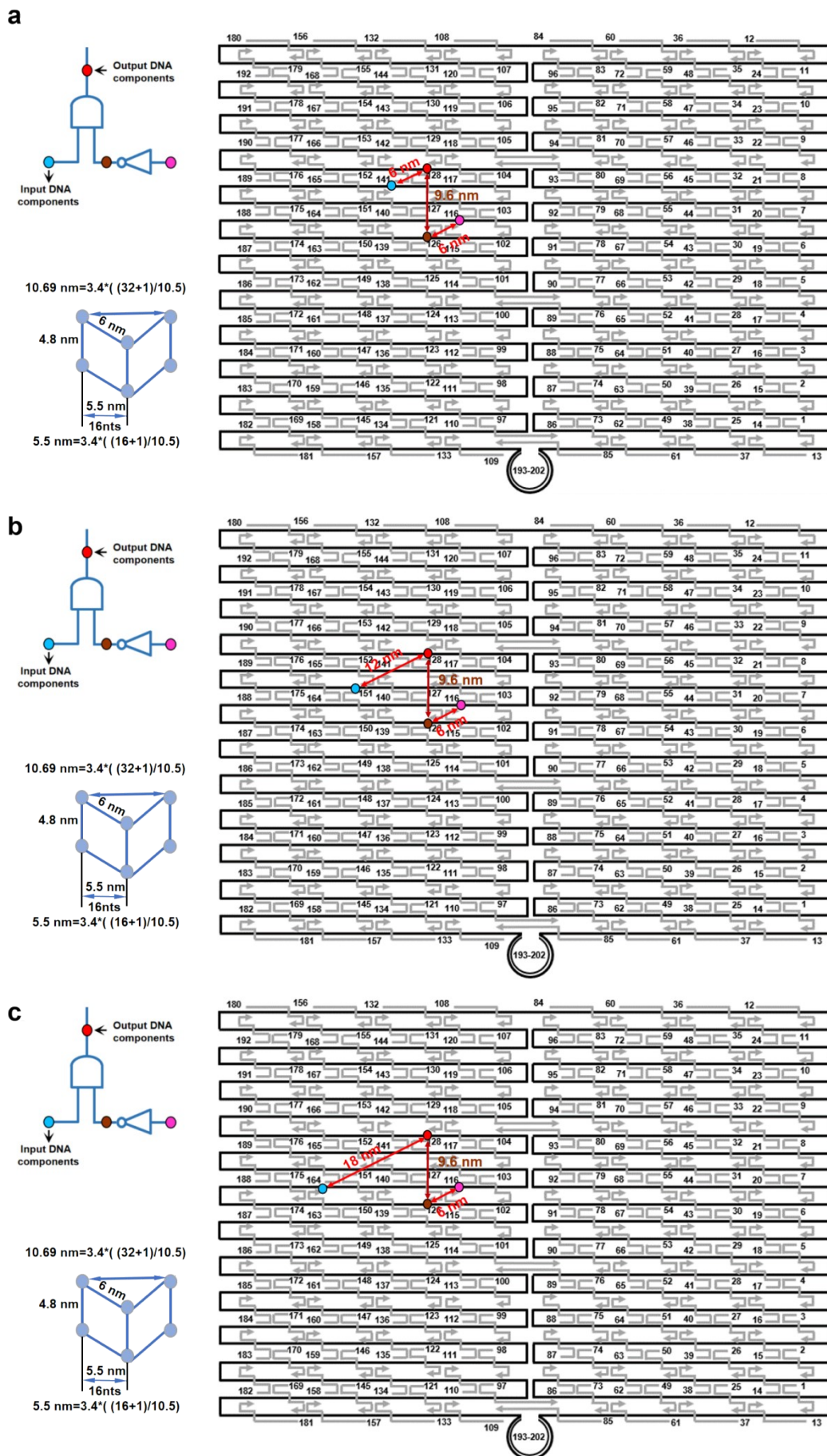


**Figure S40.** The wiring instructions of the AND-NOT logic gate with different assembly distance between Input and Output DNA components on DNA origami. (a) 6 nm; (b) 12 nm; (c) 18 nm.

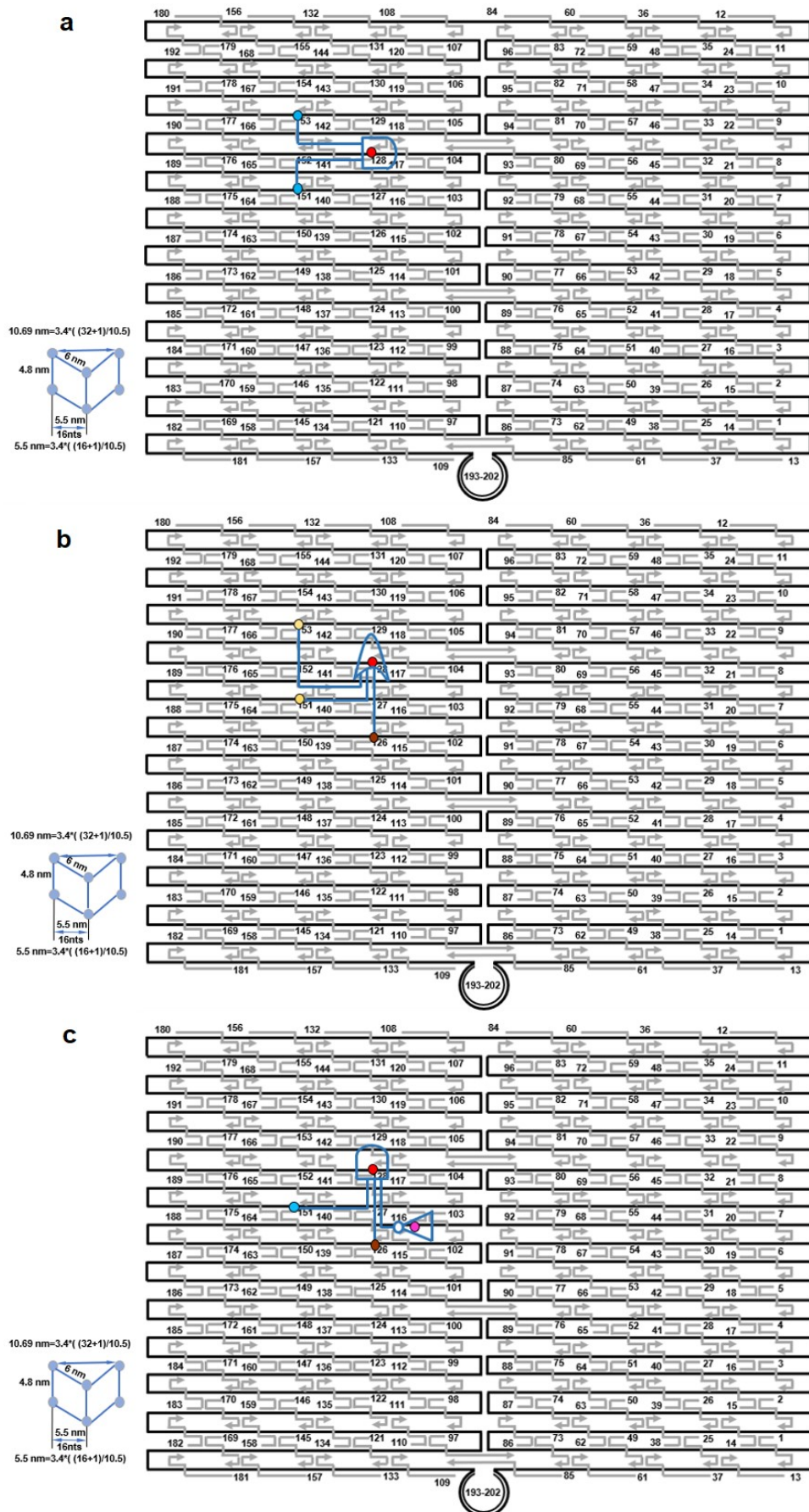


**Figure S41.** The wiring instructions of three basic logic gates on DNA origami. (a) AND gate; (b) OR gate; (c) NOT-AND gate.

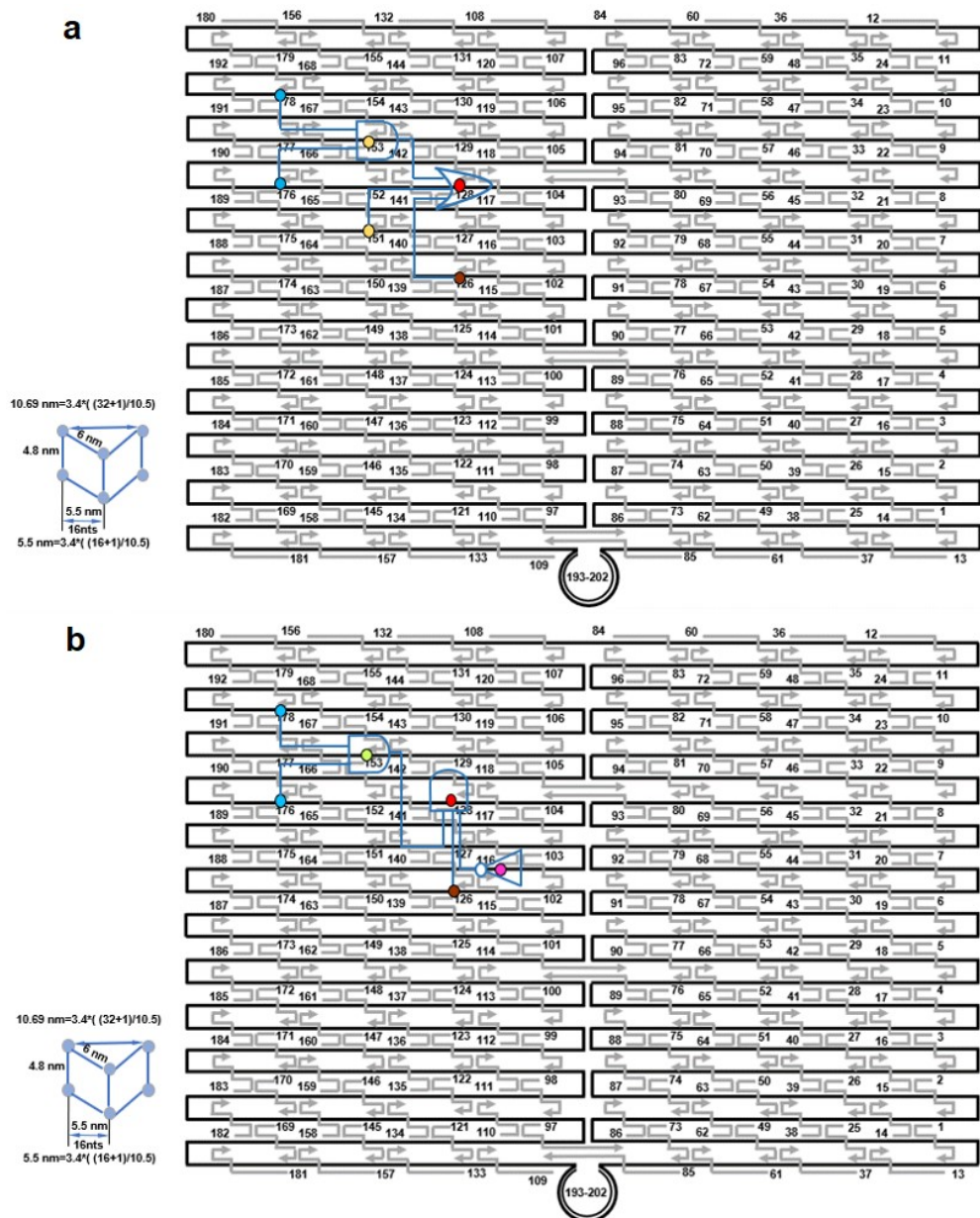


**Figure S42.** The wiring instructions of complex DNA cascade circuits on the basis of the basic AND nano-chip. (a) AND-OR nano-chip; (b) AND-NOT-AND nano-chip.





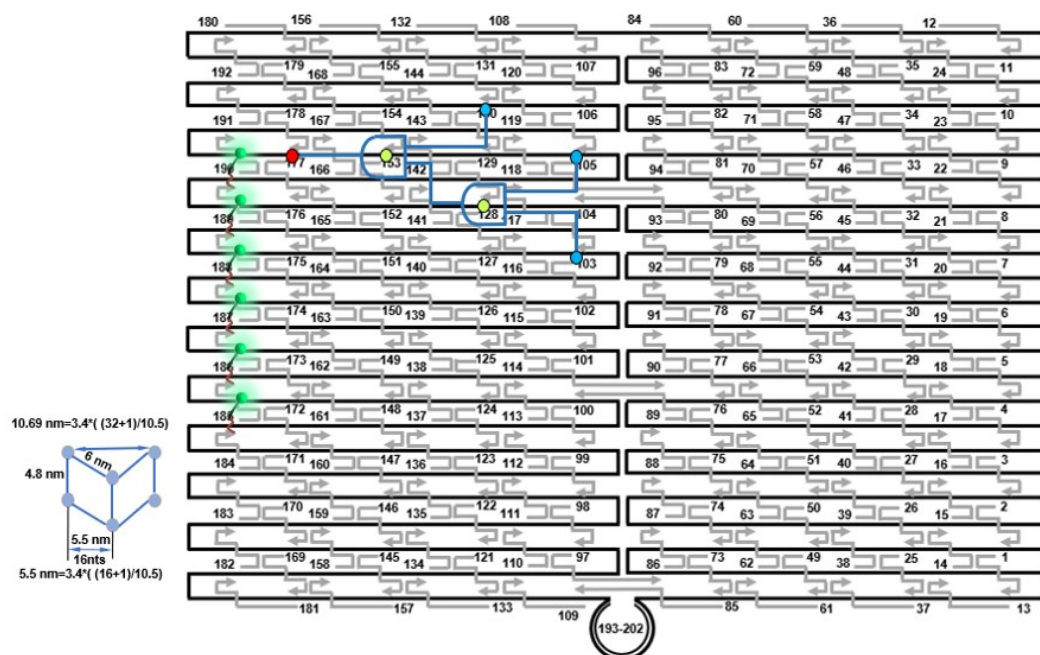


**Figure S45.** The wiring instructions of the three layers of cascade logic units on the nano-chip for intracellular molecular biocomputing.

**Table S1. Sequence of oligonucleotides used in modular logic units.**

Name	Sequence (5'-3')
A	GTAGTATTGTA CTCTGTCACGATAG
B	GTGACAGAGTACAATACTACATGACTTCGACACTACAGAT-Cy5
C	TTCACCTGATAGTACCTT(BHQ2)ATCTGTAGTGTGGAAGTCAT

A <sub>in-1</sub>	AGTGCAGGTAGCTATCGTGACAGAGTACAATACTACTTTACATCACCTATCGCTA
B <sub>in-1</sub>	ATCCATCTAGGATATCTTTTGTAGTGTGGAAGTCATGTAGTTGTAACATCC
C <sub>17-1</sub>	CACGATAGCTACCTGCACTGTAAGCACTTTG
miR-17	CAAAGTGCTTACAGTGCAGGTAG
C <sub>30a-1</sub>	CTTCCAGTCGAGGATGTTTACAACACTATG
miR-30a	TGTAACATCCTCGACTGGAAG
C-staple(128)	GGTACTATCAGGTGAAGCGTCTTTATAGCAGCCTTTACAGTAGCTATC
A <sub>in-1</sub> -staple(154)	GAAGAAAGCGAAAGGAGCGGGCGCTAGGGCGCTAGCGATAGGTGATGT
B <sub>in-1</sub> -staple(151)	GATATCCTAGATGGATATTTTATCAACAGGGAAGCGCATTATAATAAG
A <sub>in-2</sub>	CGACTGGAAGCTATCGTGACAGAGTACAATACTACTTTCTATAGGATCTACCTA
C <sub>30a-2</sub>	CACGATAGCTTCCAGTCGAGGATGTTTACA
N	CTCATGTCTCTCGTCTTACTGTAGTGTGGAAGTCATGTAGT
A <sub>in-2</sub> staple(152)	TCTGTCCAAAATAAGAATAAACACAAATATATTAGGTAGATCCTATAG
N-staple(126)	GACGAGATGACATGAGACATCACCCTAAGAATAACGTTAATGCG
C <sub>30a-3</sub>	GTCATGTAGTCTTCCAGTCGAGGATGTTTACA
D	CTCGACTGGAAGACTACATGACTTCGACACTTTTTCTATAGGATCTACCTA
D-staple(115)	ATTTTTGAAATTGTAAACGTTAATTAGCCAGCTAGGTAGATCCTATAG
A <sub>in-1</sub> -staple(152)	TCTGTCCAAAATAAGAATAAACACAAATATATTAGCGATAGGTGATGT
C <sub>122a-1</sub>	CACGATAGCAAACACCATTGTACACTCCA
A <sub>in-3</sub>	AATGGTGTGCTATCGTGACAGAGTACAATACTACTTTACATCACCTATCGCTA
miR-122a	TGGAGTGTGACAATGGTGTGTTG
B <sub>in-2</sub>	ATCCATCTAGGATATCTTTTGTAGTGTGGAAGTCATGTAGTTAGCAGCACA
C <sub>15a-1</sub>	CACAAACCATTATGTGCTGCTAACTACATG
miR-15a	TAGCAGCACATAATGGTGTGTTG
A <sub>in-4</sub>	AATGGTGTGCTATCGTGACAGAGTACAATACTACTTTCTATAGGATCTACCTA
C <sub>15a-2</sub>	CACGATAGCAAACACCATTATGTGCTGCTA
E	AATGGTGTGCTATCGTGACACTTCGACACTTTTTCTATAGGATCTACCTA
C <sub>15a-3</sub>	GTCATGTAGTCACAAACCATTATGTGCTGCTA
F	CACCTCTGAATGACGGATACTAGATGTGCT
G	CTGACAGATCTATCGTGACAGAGTACAATACTACCCTTACCAGTCTTACCTTTTCCGATTCCAGTTCACAG
H	GGTAAGACTGGTGAAGGCACGATAGATCTGTGAGCAGCATCTAGTATCCGTCATTGAG
C <sub>122a-2</sub>	CAAACACCATTGTACACTCCACACTCTG
F <sub>in-1</sub>	CCTTCGTATCGCATAGTTTAGCACATCTAGTATCCGTCATTGAGGTTGGAGTGTG
H <sub>in-1</sub>	ATGGTTGTGCTGCTCTGACAGATCTATCGTGCCTTACCAGTCATTTATCCGATTCCGATGAC
C <sub>15a-4</sub>	CAGAGCACCAAAACCATTATGTGCTGCTA
G-staple(154)	GAAGAAAGCGAAAGGAGCGGGCGCTAGGGCGCTGTGAAGTGAATCG
F <sub>in-1</sub> -staple(178)	CTATGCGATACGAAGGGGTTGAGGCTTTTCATAATCAAAAAGGCCG
H <sub>in-1</sub> -staple(177)	TCATGGAATGGATTATTTACATAACACCCTGTCATGCGAATCGGAT
A <sub>in-5</sub>	GGTGAATGCCCTATCGTGACAGAGTACAATACTACTTTCTATAGGATCTACGTA
C <sub>124a-1</sub>	CACGATAGGGCATTACCCTGCTGCCTTA
miR-124a	TAAGGCACGCGGTGAATGCC
B <sub>in-2</sub>	ACTCTTCCATTCGCTATTTTGTAGTGTGGAAGTCATGTAGTTAGCAGCACA
C <sub>15a-1</sub>	CACAAACCATTATGTGCTGCTAACTACATG
A <sub>in-5</sub> -staple(152)	TCTGTCCAAAATAAGAATAAACACAAATATATTACGTAGATCCTATAG
B <sub>in-1</sub> -staple(105)	GACGAGATGACATGAGTTTCATCATCGCACTCCAGCCAGCTTCGCTAT
B <sub>in-2</sub> -staple(103)	TAGCGAATGGAAGAGTTTCTGTATGAGGTGAATTTCTTAAGGCCGCTT
J <sub>in-1</sub>	ATGGTGTGCTGCTGCTAAGCCTATCCTTTCCGAGCTATTTTCTTACGCAATCCTTCC
C <sub>122a-3</sub>	GACGACGACAAACACCATTGTACACTCCA
J <sub>in-2</sub>	GTGCAGGTAGTCTGCTAAGCCTATCCTTTCCGAGCTATTTTCACTGCATCGTAGTCA
C <sub>17-2</sub>	GACGACGACTACCTGCACTGTAAGCACTTTG
L <sub>in-1</sub>	CATGACACATACCGAGTTTTTTCAGTGGATCGTGAACAGTATCAGTAGCTCCCTGTAGAA
C <sub>10b-1</sub>	ACACAAATTCGGTTCTACAGGGGAGCTACTG
miR-10b	CCCTGTAGAACCGAATTTGTGT
L	GTCTAAGCCTATCCTTTCCGAGCTACTGATACTGTTACAGTCCACTGAT-FAM
J	TAGCTCGAAAGGATAGGCTTAGACGACGA
K	CTCTAGTTCGTCTGCCTTTTAT(DabcyI)CAGTGGATCGTGAACAGTATCAG
J <sub>in-1</sub> -staple(173)	ATGAATATACATTTTAACAATTTACCTTTAGAAAGGAGATTGCGTAAG
J <sub>in-2</sub> -staple(171)	TAATTAAGTACCGACAAAAGGTAATAATAAGTACGATGCACTG
K-staple(147)	GCGACGCACTAGAGCGTATAATAAACAGGAGGCCGAAAAACGC
L <sub>in-1</sub> -staple(122)	CTCGGTATGTGCTATGTTGAATATCATTTCAATTACCTATTTATCA
J <sub>in-3</sub>	GGTGAATGCCCTGCTAAGCCTATCCTTTCCGAGCTATTTTCTTACGCAATCCTTCC
C <sub>124a-2</sub>	GACGACGAGGCATTACCCTGCTGCCTTA
J <sub>in-4</sub>	TGTAGCTCATCTGCTAAGCCTATCCTTTCCGAGCTATTTTCACTGCATCGTAGTCA
C <sub>143-1</sub>	GACGACGATGAGCTACAGTCTTACATCTCA
miR-143	TGAGATGAAGCACTGTAGCTCA
M	CGAGTCAGAATGTCAGATACGAGAAGTCAG
O	GAGTCATGTGCGTCTAAGCCTATCCTTTCCGAGCTACCATACCAGTCTTACCTTTTCCGATTCCAGTTCACAG
P	GGTAAGACTGGTGTAGGGACGACGACATGACTCTGACTTCTCGTATCTGACATTCTG
M <sub>in</sub>	CCTTCCTATCGCATTCTTCTGACTTCTCGTATCTGACATTCTGACTCGTAGCTTATCA
C <sub>21</sub>	TCAACATCAGTCTGATAAGCTACGAGTCAG
Control C <sub>21</sub>	TCATTATCAGTCTGATAAGCTACGAGTCAG
miR-21	TAGCTTATCAGACTGATGTTGA
P <sub>in</sub>	GTGCAGGTAGTCAAGGAGTCATGTGCGTCCATCACCAGTCTTACCTTTTCCGAGCTTCTAGTCA
C <sub>17-3</sub>	CTCCTGACCTACTGCACTGTAAGCACTTTG

**Table S1. Sequence of oligonucleotides used in modular logic units.**

Name	Sequence (5'-3')
Control C <sub>17-3</sub>	CTCCTGACCTACCTGCACTGTAAGCATCTTG
Q	TAGCTCGAAAGGATAGGCTTAGACGACGC
S	CATCGATTTCGCTGCCTTTTGTCATTGTCATCAGTGGTATCTGTCTAGAGCGTGAACAGTATGAC
R	GTCTAAGCCTATCCTTTCCGAGCTACTGATGATGTTACAGTCCACTGATGCAATGACG

R <sub>in</sub>	CATAGCACTTACCGAGTTTCGTCATTGCATCAGTGAGCGTGAACAGTATGACTAGCTTGTAACATCC
C <sub>30a-4</sub>	CTTCCAGTCGAGGATGTTTACAAGCTAGTC
Control C <sub>30a-4</sub>	CTTTTAGTCGAGGATGTTTACAAGCTAGTC
T	BHQ2-CGCGACGCTCTAGACAGATACCACCTTTTTAGTCCACACCAATCCG
Aso	GTCTAGAGCGTGCCCAT-Cy5
M <sub>in</sub> -staple(105)	GAATCGATAGGAAGTTTCATCATCGACTCCAGCCAGCTTCGCTAT
P <sub>in</sub> -staple(104)	TGGCAAGAGTCTGTCCATCACGTAGTAATATGACTAGCAAGCTCTG
O-staple(129)	GGAAGGGCCGCTCACAAATCCACGCCTGGGCTGTGAAGCTGGAATCG
S-staple(153)	GGCAGACGAATCGATGAATTAATTACAGTAACAGTACCTAATTCAT
R <sub>in</sub> -staple(130)	GAGGGTAAGTGCATATGCAGGGCCGAGGAACGGTACGCCAAGAACAAT
T-staple(178)	GGTTGAGGCTTTTCATAATCAAAAAGGCCGCGGATTGGTGTGGACT
U	FAM-TTTTTTACCATCCTATCCGACA
U-staple(184)	AAATACCGGGCAAATCAACAGTTGAGTATTAGTGTCCGGATAGGATGGT
U-staple(185)	ACCGTCCGGGGACGACGACAGTATGTGCTGCTGTCCGGATAGGATGGT
U-staple(186)	AATAAGCGGTGTCGAAATCCGCGAACTCATCTGTCCGGATAGGATGGT
U-staple(187)	ATTTCAACAACCTCGTTTACCATTGCAATGTCCGGATAGGATGGT
U-staple(188)	ATAAAAATTCAGAGCATAAAGCTAACAGTTGATGTCCGGATAGGATGGT
U-staple(189)	GTGCCTAAGTTGCCCCAGCAGGGGCAAAAATGTCCGGATAGGATGGT

**Table S2. Sequence of oligonucleotides used to synthesize DNA origami.**

Name	Sequence (5'-3')
1	AACATAAACTGAATCTTACCAACAATAGCA
2	ACCGTAATAATTCATATGGTTTACACATACAT
3	ATATATGTATCAATATGATATTCAAGACAGTC
4	GACGCTGACTGATGCAAATCCAATAGTATCAT
5	ATCCTTTGATTATCAGATGATGGCTTTACATC
6	CAGTTTGAGATTCTCCGTGGGAACAATCAGAA
7	CACCACACTTTTTATAATCAGTGAACCTCAAAC
8	GAGGCTTTCATTAACGGGTAACCAACTT
9	TTTGAGTCAGAAAGGAGCGGAATTGATTGCT
10	CTGCAACAATCTAAAGCATCACTTTAAAAG
11	CAAGAACAACAAGCAAGCCGTTTCAGTTACA
12	GCCTGGCCTCACTGCCCGCTTTGAATTCGT
13	GATTAGCGGGTTTTGCTCAGTACCAGCGCGGA
14	AAAGGTGGAATTGAGTTAAGCCCAAGACGGGA
15	ATCGATGATGTACCCCGGTTGATAAACGGC
16	AACCTGTTGAGAGTACCTTTAATTAAGACTT
17	ACCTCAAATGAGGCGGTCAGTATTTGCCAGAT
18	ATGCAATCAAAGAATTAGCAAATTTAGTTT
19	CAATATAAAAACAATTCGACAACCTAATATCT
20	GTGAGACGTCGTGCCAGCTGCATTTGACTCT
21	TAGTAGTAGGTGAGAAAAGCCGGACCGTTC
22	ATAAAGCCTTTTAGAACCCTCATATATCAGGT
23	TATTCCTGCCCGAACGTTAATATCTTGCTGA
24	GAGAAGTGCCGCGCGCTTAATGCGCCGCTA
25	TTACCGAAATGATTAAGACTCCTTCGATTGAG
26	ATTACCGCCACACGACCAGTAATAGAAGATAA
27	ACGAGTAGAACGGAGATTTGTATCGCGCGAAA
28	CGCTGAGGCAGCGATTATACCAAATCGCCT
29	GAAAGCCGAAATCAAAAAGAAATAGCCAAGCGGT
30	TATCGGCCCAACAGAGATAGAACGCCATTAA
31	CAACTAAAATCTCCAAAAAAGGCTACA
32	TCACCAGTCAGCCATTGCAACAGGTTAAAGGG
33	TCTAAGAAAAGTCTGAACAAGAAAAAGTAAT
34	CAAAAAGCTGGATAGCGTCCAAATAACGCC
35	GAGGCAATCGTCACCCTCAGCATATCAGCT
36	GGGTTGAGGCCCCCGATTTAGAGCTTGACGGG
37	GGCATTTCAAATAAATCCTCATTAAAGCCA
38	TAATCTTGAAGGGAACCGAACTGAATACGTAA
39	CAGGATTATAGCTATATTTTTCATCTACTAA
40	GGGTAATTTAAATTTGGGCTTGAGAACCCAGA
41	CCGACTTGTGCAGAACCGCCTGTCAACATGT
42	ATATTTAGAGATCTACAAAGGCTATTTTAA
43	CCACAAGCAACATATAAAAAGAAATCACAATC
44	TGATAAGAAGATACATTTTCGCAAAAATCATA
45	TTCCCAATTGCTGAATATAATGCTTTACCCTG
46	AGAGGATCTAAGTTGGGTAACGCCGATCTGC
47	ATATTTTGCATAACTTCTTTGATCAAATTA
48	CTGTTTGAAGCATAAAGTGTAAAACAACATA
49	TGCCACTAGAACGAGGGTAGCAACGGCTCCAA
50	GAGCCGCCCTCAGAGCCGCCACCAGAACC
51	AAGATTATGAACACCCTGAACAGAGATAAC
52	TTGACCCCTTGCAGGGAGTTAAAACAGCTTG

**Table S2. Sequence of oligonucleotides used to synthesize DNA origami.**

Name	Sequence (5'-3')
53	AACAGAGGTATCAAACCTCAATCCGATTTAA
54	ACAGTTTCTTTAATTTGATCGGTTGCGAAAAGA
55	TGCTTTCCGGATTTTGTAAACAACCTTTCA
56	GCCATTCGTAACCAATAGGAACGCAAAATCAGC

57	ACCACATTTGGGAAGAAAAATCTAATCAAGAG
58	AATAGAACAGTAGCGACAGAATTTTCATC
59	GTCCTACTCGTAAAGCACTAAATCGAACCCCT
60	ACCGCTTCGGCTCTGGCCTTCCTGATTTTGTT
61	GGTTGATATAAGTATAGCCCAGGAATAGGTGTA
62	ACTTTACATCCTGATTGTTTGGATAACGTCAG
63	CCTTTAGCGAATAAGTTTATTTTGACGCAAAG
64	AAATGAAACCAGAGCCTAATTTGCTTATTTTC
65	CCGTTGTATGGTGGTTCCGAAATCCGAAAATC
66	AACATGTTGTTTCATTCCATATAAAATCGGT
67	GAAACGTCAGGGCGACATTCAACATTACGC
68	GAATTAACGTTGCTATTTTGCACCTCCGGTAT
69	TCATTTTTTTTGCACGTAAACAGTACCATAT
70	ATGCGTTAGCATTTTCGAGCCAGTTAGAACC
71	AAAATTCGAAATTAATGCCGGAGAGGTAAGA
72	ATACCGATTTTCCAGACGTTAGTAAATGAATT
73	AAAAGGAAAGAACTGGCTCATTCAATACCC
74	TCAGCTAAGAAATACCGACCGTGTCTAAATTT
75	ACCACCAGCCACCACCGAAACCGCGCAAATC
76	AGTATGTTACAATGAAATAGCAAAGAGAAT
77	TTCAAAGGCATTAACATCCAATATGGTCAAT
78	AAATTGCTAATGAAACAGTACTTCTGTAA
79	AATAGATCGCGAGGCGTTTTAGCTTAAATC
80	CGAACCGAAAATAGCGAGAGGCTGACGACGA
81	ATTTTAGAGTACTATGTTTGCTTTGACGAGCA
82	CAAATATCTTGCCAGAGGGGTAAGAGCAAC
83	GGATAGCAAGCCCAATAGGAACCCATGTACCCTAACACTG
84	AAATGCTTCAAAAATCAGGTCTGTAGCTC
85	CAACGCTTAAACAACGCCAACATATCATTCC
86	ATAGCCGCAATAATAACGGAATAATTATTC
87	AAAACGAATTCATCAGTTGAGATCCCCCTC
88	GACCATTGGTCATTTTTGCGGAGATTGCAT
89	TCCCTTATGCGAACGTGGCGAGAAAGGAAGG
90	AGGCAGAGTACAAATCTTACCAGTAACTATA
91	GAAACCTGGGCAACAGCTGATTGCGAACCAAGA
92	TGTTTGAATTAAGAGGAAGCCCGGCTCCTTT
93	CAAACCTACAACGCCTGTAGCATTCCACAGACA
94	CCACGCTGTGAGTGAGCTAACTCAGTGTGAAA
95	ACTATTATTAATATTCATTGAATTTAGGAAT
96	AAAGGGATGTTGTTCCAGTTTGCCTTCACC
97	ATCGTCGATTTTCATCTTCTGACGATAAATA
98	AAGAAGTTGCGTTTTAATTCGAGAACAGGT
99	TTGTCTCAGTTGCGCCGACAATATTCGGT
100	TACGCCAGGTCATAGCTGTTTCCTCATTAATT
101	AACCAGAGAGCCGCCCCAGCATTGACAGGA
102	GGATTGACGCGCATCGTAACCGTAGGGTTT
103	TTCTGTATGAGGTGAATTTCTTAAGGCCGCTT
104	TGGCAAGAGTCTGTCCATCACGTAGTAATA
105	TTTCATCATCGCACTCCAGCCAGCTTCGCTAT
106	ACCAGTAGGGTAAATATTGACGGAACCCAAAA
107	TGAGGAAGATAGCCCTAAAACATCCCTTCTGA
108	ATGTTACTCGTAACAAAGCTGCTCTACCTTAT
109	CGAGCTGAACCGGAAGCAAACCTCCCTTCAAAG
110	CCATCGCCAGTTAGCGTAACGATCTAAAGTT
111	AAGCCCAAGAGAGTCTGGAGCAAAAACGCAAGG
112	AGTAAAAGTGTAGCGGTCACGCTGCGCGTAAC
113	CATTGCCATAAACAGGAAGATTGTGAGTAACA
114	CAGCATCGGAAGGCACCAACCTAGCAGACGG
115	ATTTTTGAAATTGTAACGTTAATTAGCCAGC
116	GCGTTGCGCCTGAGAGAGTTGCAGCCGAGATA
117	GAACCTGGCGCCCTTTTTAAGAAAAACGTCAA
118	TGAATAATCATTGAGGATTTAGAAAAGGAAT
119	AAGACAAAACCAATGAAACCATCGTATTAGCG
120	ACACCACGGAGCGCTAATATCAGAAAGTCAGA
121	TCCCATCCAGATATAGAAGGCTTACAGCTACA
122	TTGAATATCATTTCATTACCTATTTATCA
123	AATCATGCTGGCGAAAGGGGGATCGGCCTC
124	TGCCCCCTGCCTATTTCCGGAACCTATTATTCT
125	CGAGCCGGCCATTACGGCTGCGCAGGCAAAGC
126	ACATCACCGTAAGAATACGTGGTTAATGCG
127	TTGCGGAAAGAATACACTAAAACCTGCTCC
128	GCGTCTTTATAGCAGCCTTTACAGTAGCTATC

**Table S2. Sequence of oligonucleotides used to synthesize DNA origami.**

Name	Sequence (5'-3')
129	GGAAGGGCCGCTCACAATCCACGCCTGGG
130	CAGGGCGCCAGAACGGTACGCCAAGAACAAT
131	CTCTGAATTTACCGTTCCAGTAAGCGTCATAC
132	ACCTTTTGTAGATTTTACAGTTTTATACTTC

133	GCGATTTTATTACGAGGCATAGTATAGTAAAA
134	AATGGTTTGAGTGAATAACCTTGCATAAATCA
135	AAATCAATAGCCGGAACGAGGCAAACGAAA
136	ACTATCATTTTAATCATTGTGAATATTAGTG
137	AATAATTCTGGTGCCGGAACCAACTGTTG
138	CGGCCAACCCAGGGTGGTTTTTCTCCAACGT
139	AATCAATAAATCATTACCGCGCCCGCTAACGA
140	GAATATAAAGAAAAAGCCTGTTTCGCAAGA
141	GGTCAGTTAACGAACCACCAGCAAAGGGA
142	TGAAAGAGGGCTGGCTGACCTTCCGTTAAT
143	AGGCGTTGACGACGACAATAAATTATCAAC
144	TGTAATGGAAGAGTCAATAGTGAGAGCAAAA
145	GATAAATTTTCCCTGACGAGAATGGTTTA
146	TGATGATACAGGAGTGTACTGGTAATAAGTTT
147	CGTATAATAAACAGGAGGCCGAAAAACGC
148	CATTCTGGTTGCTGGTAATATCCGAATCCT
149	TAGCTGATCATTAAATTTTTGTTTCATCAA
150	AAAGTATTAAGAGGCTGAGACTCCTCAAGAGA
151	ATTTTATCAACAGGGAAGCGCATTATAATAAG
152	TCTGTCCAAAATAAGAATAAACACAAATATAT
153	AATTAATTACAGTAACAGTACCTAATTCAT
154	GAAGAAAGCGAAAGGAGCGGGCGTAGGGCGC
155	AGCTTAATTCTGCGAACGAGTAGAATTAAGCA
156	TCCAGTCTTGATGCCTGCAGGAATGAAT
157	CAAAGGGCACCAATCAAGTTTTTTGGGGT
158	CACTAACAGAATGGCTATTAGTCTCACAGACA
159	GGAGGGAACACCATTACCATTAGCATCACCGG
160	GTTTAGTACCGCCACCCTCAGAACGCCACCCTCAGAACC
161	CGAGGTGCTTAAAGAACGTGGACTTTTCACCA
162	AAGGAGCCAGCGGAGTGAAGTGAAGGAA
163	CAAAGAACAACATAGCGATAGCTAAAACAA
164	ATCGTAGGATCGGCTGTCTTTCCTTGTAATTT
165	CGAACTGGTTATCTAAAATATCCGTCATA
166	TTTGCCATCAGGTCAGACGATTGGCCTTGATA
167	CCTGAAAGTTGCCTGAGTAGAAGAGGCCACCG
168	AGCAAGAAAGCAAACGTAGAAAATCAGCGCCA
169	AATCGTCAAGTCAGAAGCAAAGCGTGGCTTAG
170	AGCAAATCTAATTTACGAGCATGAATAAGA
171	TAATTACTAGTACCGACAAAAGGTAATAATA
172	TAAAAACCCGGGAGGTTTTGAAGCCGAACCTC
173	ATGAATATACATTTAACAATTTACCTTAGAA
174	TCAATCATAACAAGAACCGGATATTATACCAGT
175	AAGGCGATCCCGGGTACCGAGCTCCAGTCGG
176	AGGCAAGGGCCTGAGTAATGTGTAGGGTAGCT
177	TCATGGAATGGATTATTTACATAACACCCGC
178	GGTTGAGGCTTTTCATAATCAAAAAGGCCG
179	TCCTTGAAAGCGAGAAAACTTTTCCGGAATCA
180	TTCACAAATCGGTCATAGCCCCCTATAGCAGC
181	TCAGTGCCTTGAGTAACAGTGCCCGTATAAAC
182	GAAGATGACAATAACGGATTTCGCCTATCATCA
183	GAATGGAAGTCAGACTGTAGCGCGCAAGTTTG
184	AAATACCGGGCAAATCAACAGTTGAGTATTAG
185	ACCCGTCGGGGGACGACGACAGTATGTGCTGC
186	AATAAGGCGTGTGAAATCCGCGAACTCATCT
187	ATTTCAACAACCCTCGTTTACCATTGCAA
188	ATAAAAATTCAGAGCATAAAGCTAACAGTTGA
189	GTCCCTAAGTTTGCCCCAGCAGGGGCAAAA
190	ATTAAAGTGGGAATTAGGCCACTCCCTCA
191	AAATAAAAACGATTTTTTGTGTTGTAAGCAG
192	GATAATAGGAAGGGTTAGAACCAATAAAG
193	TTTAGTTACTATTAATTAATTTTCTTTGAATT
194	GGGAGAAATGAAACAAACATCAAGTAGATTAA
195	CAAAATTAACATAATAGATTAGAGCTTAGGAG
196	TGTACCAAGAAGCCTTTATTTACAAGAGA
197	AGGAAGAACATTAATGTGAGCATAAGCAA
198	TTGTTATCGATCGGTGCGGGCCTTTCCGGC
199	CAGGACGTCAACTAATGCAGATACTACTCGCG
200	AAATCATTTAGGTTGGGTTATATATAAAGC
201	CAAAGTACCACGCATAACCGATATGACAACAA
202	AAATCACCAAAGGTGGCATCAATTTGGGGCG